

NASA CONTRACTOR
REPORT

CR-61164

CR-61164

FACILITY FORM 802

N67 17632

(ACCESSION NUMBER)

(THRU)

57

(PAGES)

(CODE)

CR-61164

(NASA CR OR TMX OR AD NUMBER)

07

(CATEGORY)

SINGLE PARAMETER TESTING
PHASE E

Prepared under Contract No. NAS 8-11715 by
E. L. Berger, C. A. Grunden, and J. T. Sterling

GENERAL ELECTRIC

GPO PRICE \$ _____

CFSTI PRICE(S) \$ _____

Hard copy (HC) 3.00

Microfiche (MF) .65

ff 853 July 65

For

GEORGE C. MARSHALL SPACE FLIGHT CENTER
Huntsville, Alabama February 1967

February 1967

CR-61164

SINGLE PARAMETER TESTING

PHASE E
(Dated July 1966)
Part III

By

E. L. Berger, C. A. Grunden
and
J. T. Sterling

Prepared under Contract No. NAS 8-11715 by

GENERAL ELECTRIC
Apollo Support Department
Daytona Beach, Florida

**Distribution of this report is provided in the interest of
information exchange. Responsibility for the contents
resides in the author or organization that prepared it.**

NASA-GEORGE C. MARSHALL SPACE FLIGHT CENTER

ABSTRACT

This report documents the work performed on the single parameter testing program during the first quarter of Phase E, Contract NAS 8-11715, Part III. The objective of single parameter testing is to simultaneously determine several individual parameters of a component or system, thereby obtaining faster checkout time. The objective of Phase E is to apply the single parameter testing techniques developed in previous phases to an AC and also a DC amplifier. The amplifier characteristics to be measured are the frequency response and the amplifier linearity.

The areas covered in this quarterly report are:

- 1) the investigation of simpler test signals
- 2) the AC amplifier analysis
- 3) a transfer function determination program
- 4) the measurement of nonlinear component parameters.

TABLE OF CONTENTS

Section		page
1.0	INTRODUCTION	1-1
2.0	TESTING SIGNAL SELECTION	2-1
3.0	NONLINEAR SYSTEM TESTING ANALYSIS	3-1
4.0	AC AMPLIFIER ANALYSIS	4-1
5.0	TRANSFER FUNCTION DETERMINATION PROGRAM	5-1
6.0	CONCLUSIONS	6-1
	REFERENCES	6-2

1.0 INTRODUCTION

This report documents the work performed on the single parameter testing program during the first quarter of Phase E, Contract NAS 8-11715, Part III. The objective of Phase E is to apply the single parameter testing techniques developed in previous phases to an AC and also a DC amplifier which are used as signal processors between the space vehicle transducers and the telemetry equipment. The amplifier characteristics to be measured are the frequency response and the amplifier linearity.

The objective of single parameter testing is to simultaneously determine several individual parameters of a component or system, thereby obtaining faster checkout time. A block diagram of the implementation of the time sampling technique is shown in Figure 1-1. The input probing signals for electrical equipment testing can be stored in a memory device or generated with digital or analog circuitry, for example, the generation of a pulse. The estimator, timing control, and sample and hold circuits are programmed on an analog computing device such as a small commercially available analog computer or a specially designed group of analog computer components. The function of the reference response block in the diagram can be performed in three different ways. It can be a reference response of a nominal system recorded on the memory device, or a model of the nominal system implemented on the analog computing device or third, a nominal component. For the second and third way, the input probing signal is fed to the model (or nominal component) as well as to the component to be tested.

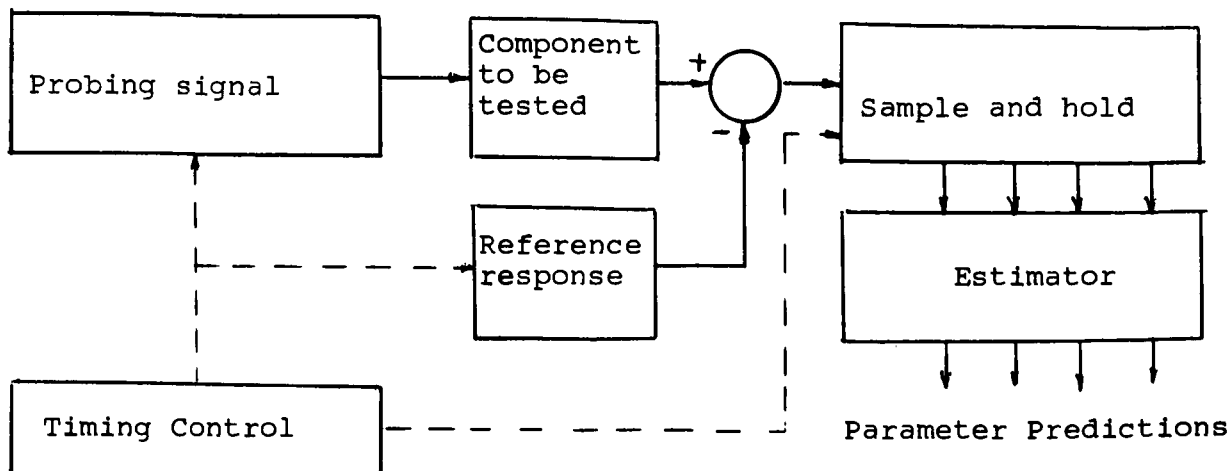


Figure 1-1

Testing Using Growing Impulse Response Probing Signals

An outline of the steps necessary to implement the technique is:

- 1) Develop a component model of a nominal component which can be used in the determination of an estimator.
- 2) The estimator is then determined by methods described in the Phase C report (Reference 4)
- 3) The third step is the implementation and checkout of the technique with the actual hardware to be tested.

Section 2 of this quarterly report describes an investigation of the improved testing signals for single parameter testing. Previous work has used growing exponential signals and growing impulse response testing signals. In this quarter, signals such as pulses, ramps and others were evaluated. Using these testing signals which are simpler to generate, the parameter prediction results obtained were comparable to previous results reported in

the final Phase C report (Reference 4). Section 4 discusses the results obtained in measuring the coefficients of a polynomial nonlinearity and nonlinear characteristics such as limiting and dead-band. The analysis of the AC amplifier to determine a nominal model is presented in Section 4. The DC amplifier analysis will be performed during the next quarter. Section 5 describes a digital program which accepts sinusoidal magnitude and phase data as input and gives the best (in a least square sense) transfer function to fit the data.

Conclusions for this quarterly report are given in Section 6.

2.0 TESTING SIGNAL SELECTION

Several input testing signals were evaluated during the quarter to determine if the same parameter prediction information could be obtained using simpler testing signals than previously investigated. Among the signals considered were

- 1) a pulse
- 2) a ramp (1 cycle)
- 3) a square wave (1 cycle)
- 4) a triangular wave (1 cycle)
- 5) an exponential waveform
- 6) a double pulse
- 7) a sine wave (1 cycle)

It is relatively easy to generate and control the timing of these signals. The equipment needed is digital logic cards and analog circuitry or some commercial signal generation equipment. The conclusion reached was that these simplified testing signals could be used to obtain parameter prediction results comparable to results previously presented in Reference 1. No strong preference was found for any one of the above testing signals for a general testing situation. The square wave and ramp worked somewhat better for testing low-pass and bandpass filters and the pulse was a good testing signal for a highpass filter. The frequency content of each of these signals is given in Figures 2-1 to 2-7. The timing (for example, pulse width) of the testing signal can be selected using these figures so as to put the maximum amount of signal

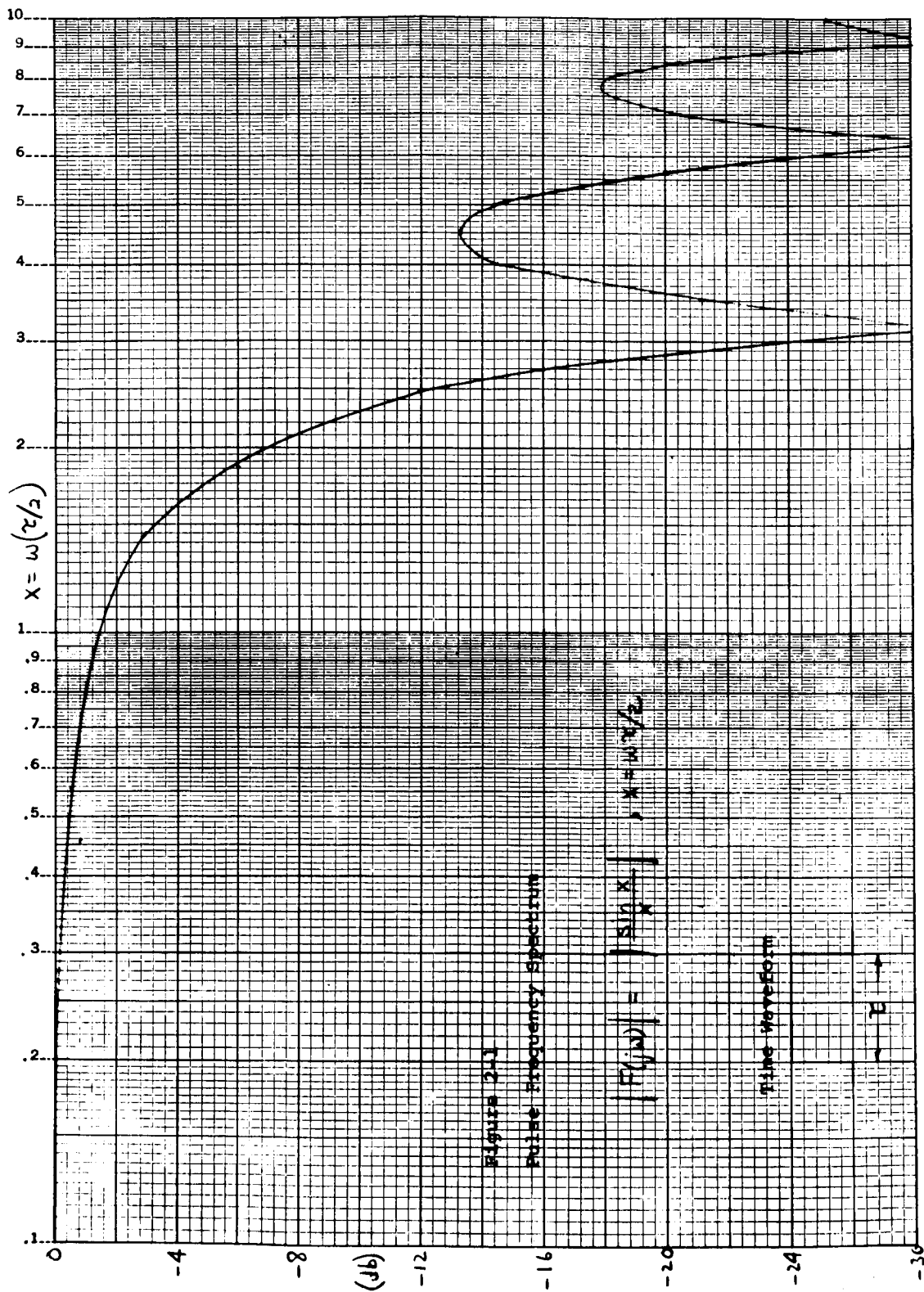


Figure 2-1. Pulse Frequency Spectrum

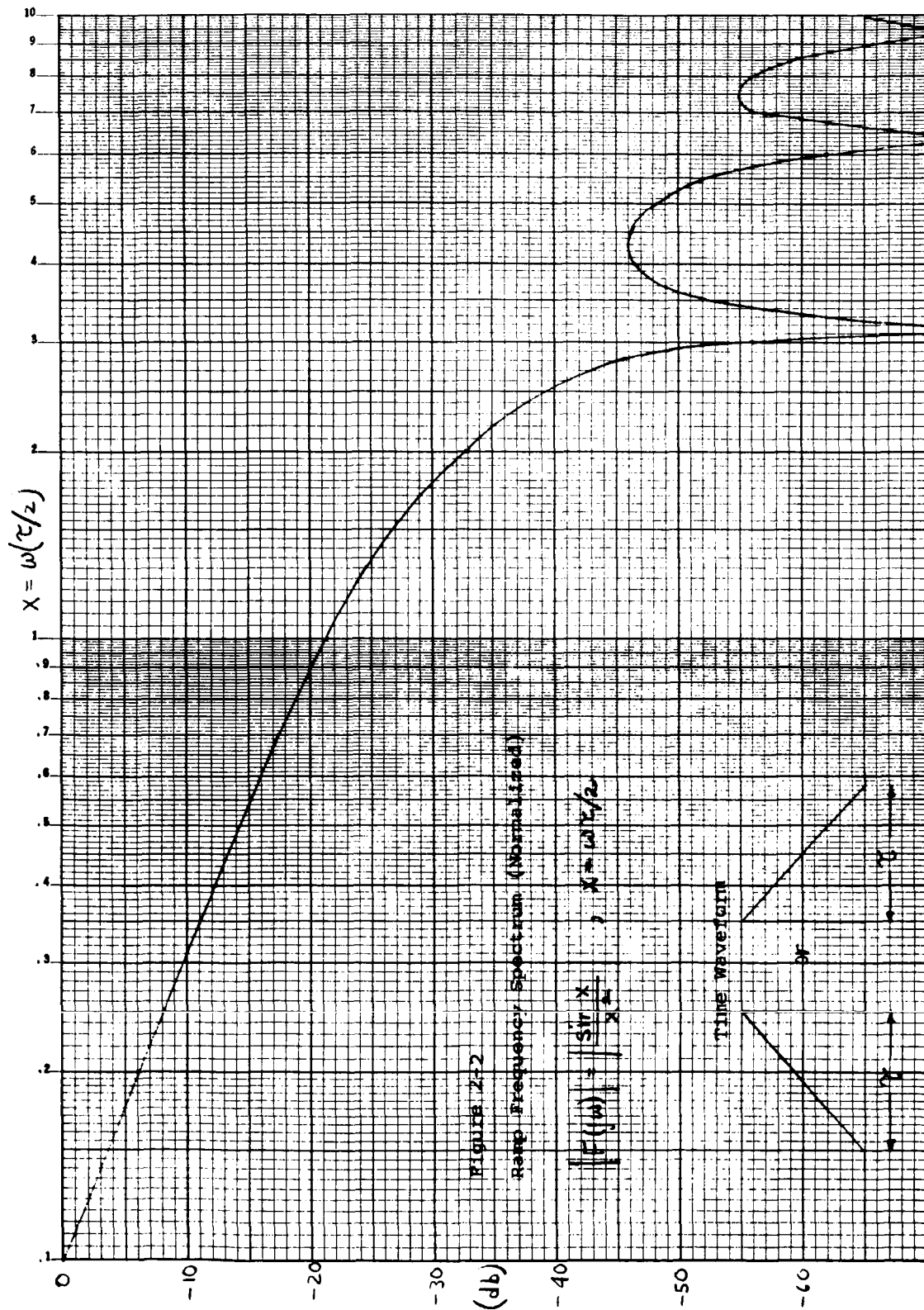


Figure 2-2. Ramp Frequency Spectrum (Normalized)

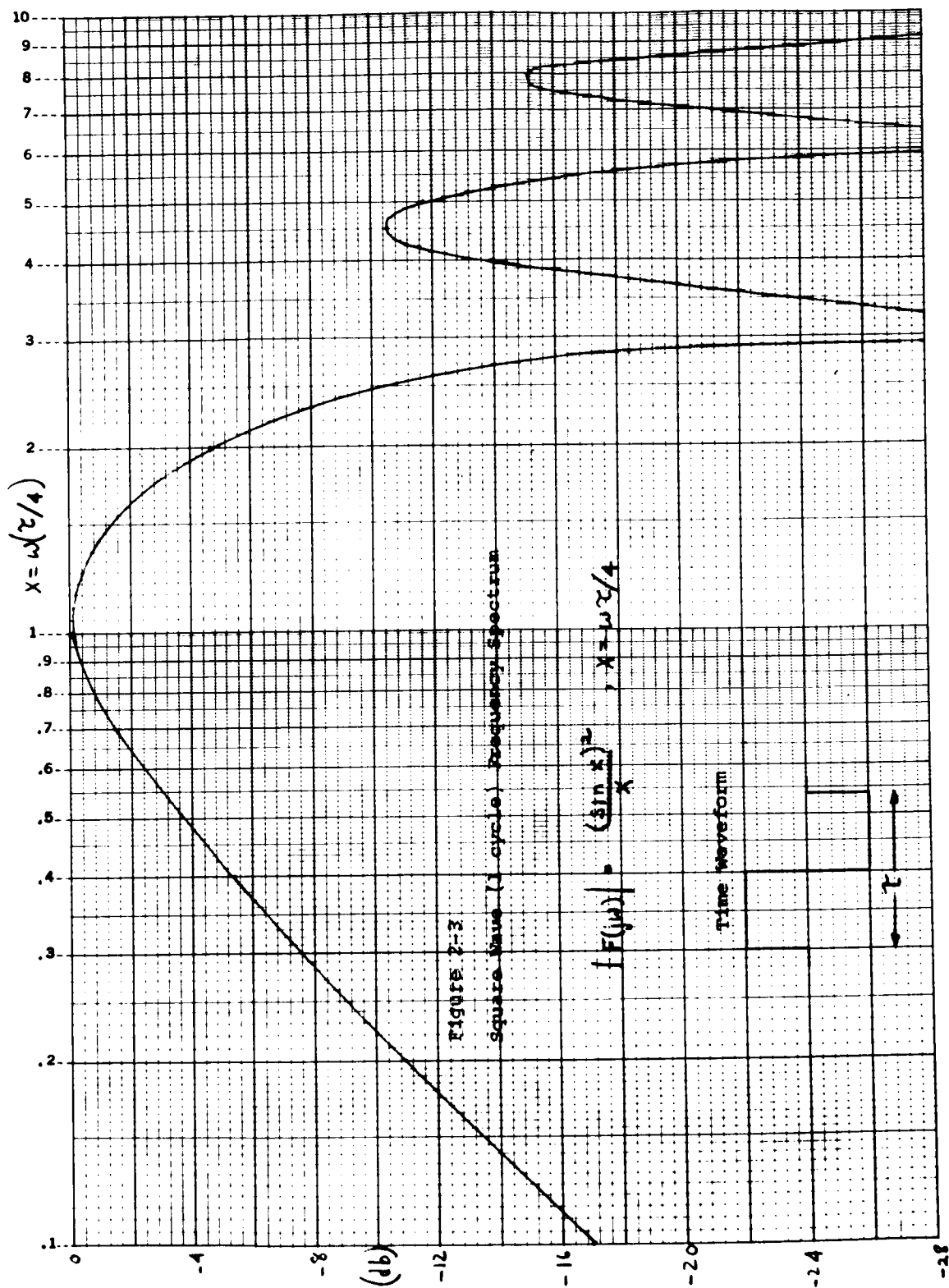


Figure 2-3. Square Wave (1 cycle) Frequency Spectrum

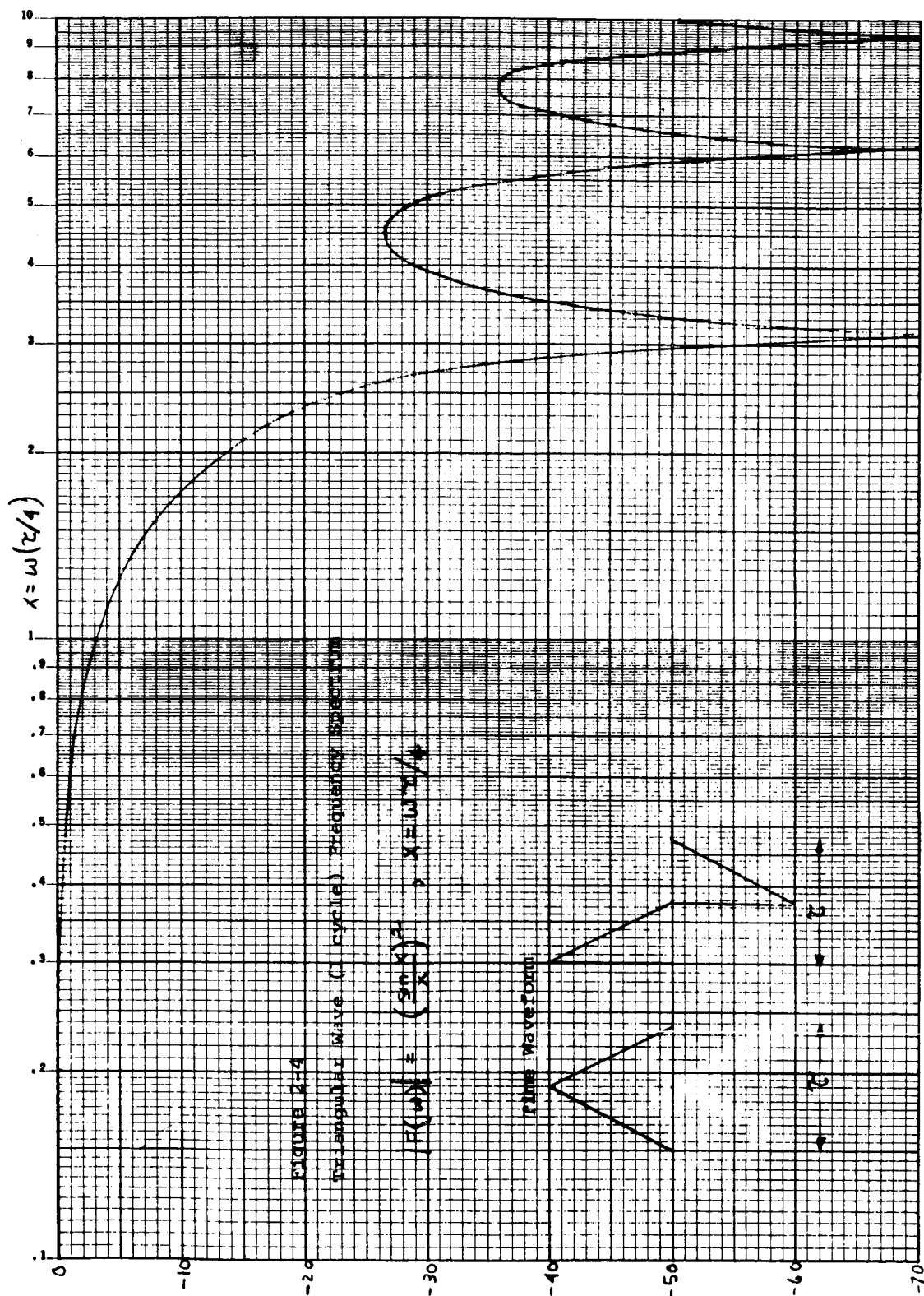


Figure 2-4. Triangular Wave (1 cycle) Frequency Spectrum

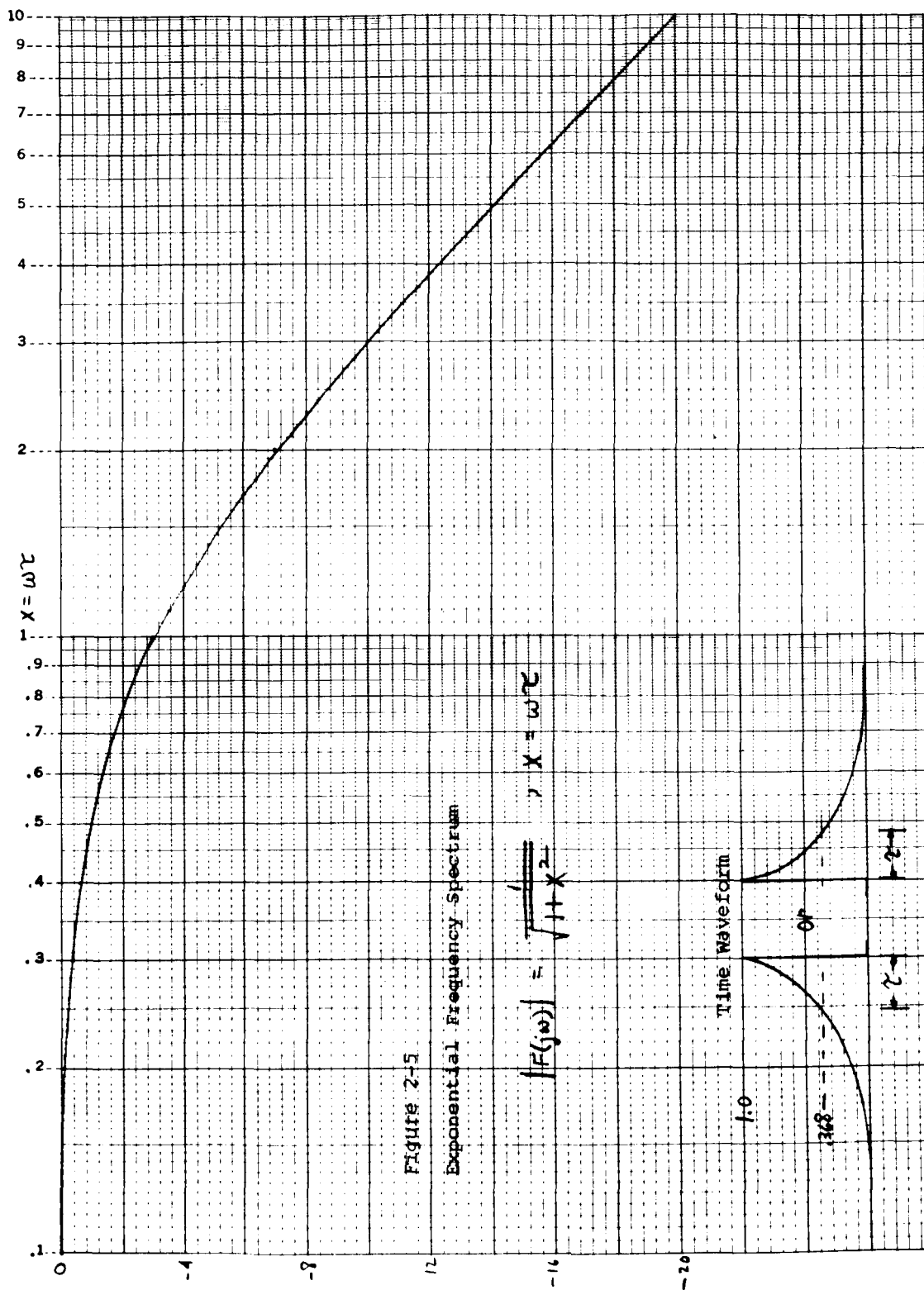


Figure 2-5. Exponential Frequency Spectrum

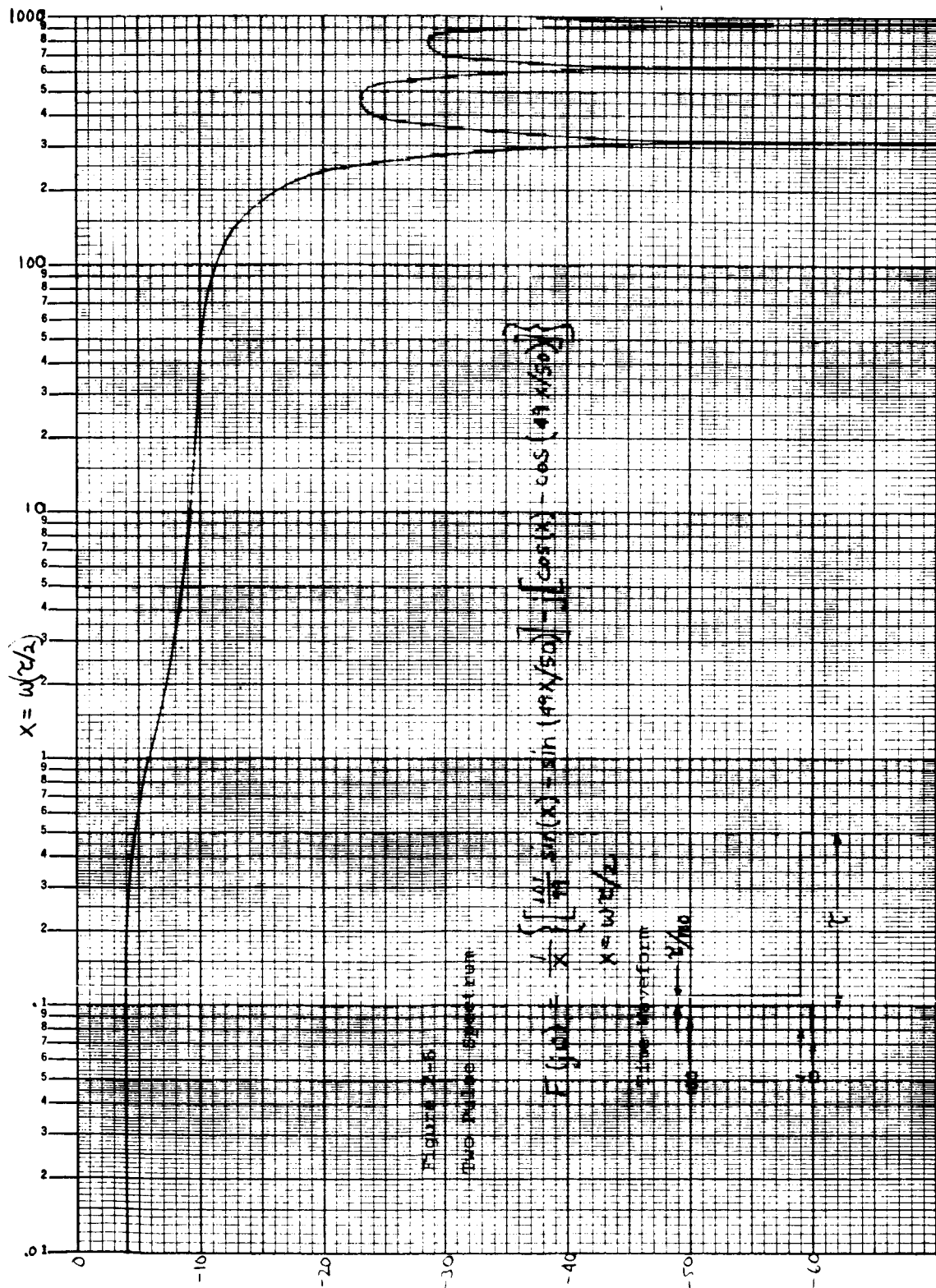


Figure 2-6. Two Pulse Spectrum.

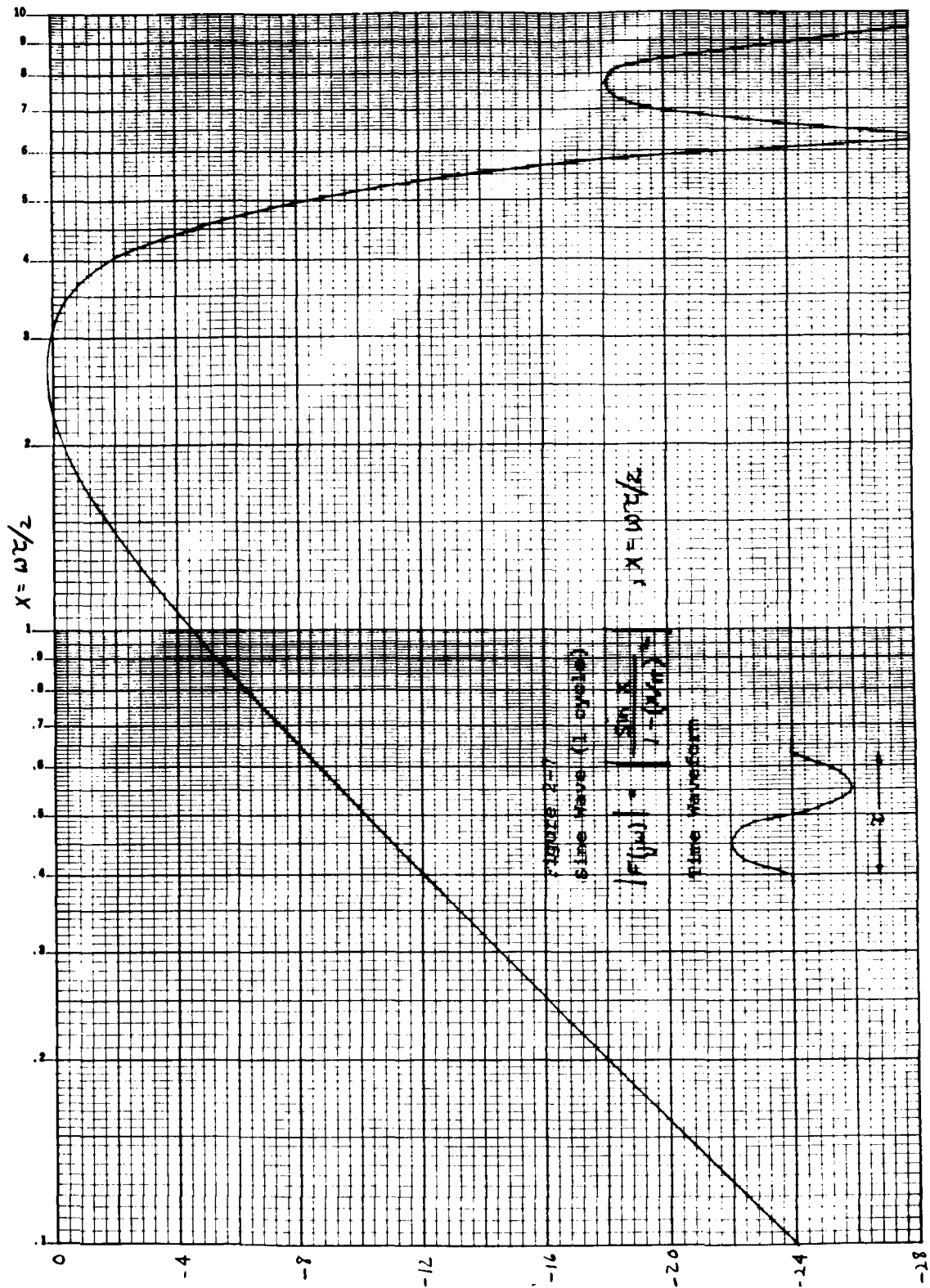


Figure 2-7. Sine Wave (1 cycle)

energy in the region of the frequency response where the component transfer function poles are located. If the poles to be measured are far apart in the frequency spectrum, two sequential testing signals may be required to measure the pole locations. Another possibility is a combination signal such as the double pulse spectrum shown in Figure 2-6. This particular signal would be suitable to measure a component with a transfer function of

$$\frac{S}{(1 + \tau S/2)(1 + \tau S/200)} \quad (2-1)$$

The sharp initial pulse in the input time waveform would measure essentially just the pole at $200/\tau$ rad/sec and the long pulse for τ seconds would measure just the pole at $2/\tau$ rad/sec.

2.1 SECOND ORDER TERMS

A factor which was given further consideration during this phase was the inclusion of higher order terms in representing the output difference waveform as a function of the parameter changes. The difference voltage waveform between the nominal system and the system to be tested (assuming two parameters that vary) can be represented by

$$\begin{aligned} V(t) = & a_1(t) X + a_2(t) X^2 + a_3(t) X^3 + \dots \\ & + b_1(t) Y + b_2(t) Y^2 + b_3(t) Y^3 + \dots \\ & + c_{11}(t) XY + c_{12}(t) XY^2 + c_{21}(t) X^2 Y + \dots \end{aligned} \quad (2-2)$$

where $V(t)$ = the difference waveform as a function of time

$$X = \frac{10\Delta P_1}{P_1}, \quad Y = \frac{10\Delta P_2}{P_2}$$

P_n = the nominal value of parameter n

ΔP_n = the change in value of parameter n

a, b, c = the coefficients

The most significant terms in equation 2-2 are the a_1 and b_1 terms, and past effort has been based primarily on these linear terms. In studying the thrust vector control system in Phase C however, one second order term (a_2) was included. During this past quarter the c_{11} crossproduct term was included to try to increase the accuracy.

Run	X	Y	$V(t_1)$
0	0	0	0
1	1	0	+40
2	-1	0	-40
3	0	1	+40
4	0	-1	-20
5	1	1	+75
<p style="text-align: center;">Table 2-1</p> <p style="text-align: center;">Coefficient Determination Data</p>			

The coefficients a_1 , a_2 , b_1 , b_2 and c_{11} for a given time t_1 , can be determined from data such as given in Table 2-1.

Assuming the experimental data given in the table, the coefficients at time t_1 would be:

From Run 1 and 2

$$\begin{aligned} V(t_1) &= 40 = a_1(1) + a_2(1)^2 \\ -40 &= a_1(-1) + a_2(-1)^2 \end{aligned}$$

implying that $a_1 = 40$ and $a_2 = 0$. From Run 3 and 4

$$\begin{aligned} V(t_1) &= 40 = b_1(1) + b_2(1)^2 \\ -20 &= b_1(-1) + b_2(-1)^2 \end{aligned}$$

implying that $b_1 = 30$ and $b_2 = 10$. From Run 5

$$\begin{aligned} V(t_1) &= 75 = a_1(1) + a_2(1)^2 + b_1(1) + b_2(1)^2 + c_{11}(1)(1) \\ 75 &= 40 + 0 + 30 + 10 + c_{11} \\ -5 &= c_{11} \end{aligned}$$

Taking data at five time points, the coefficients for five equations of the form

$$\begin{aligned} V(t_n) &= a_1(t_n) X + a_2(t_n) X^2 + b_1(t_n) Y \\ &+ b_2(t_n) Y^2 + c_{11}(t_n) XY \end{aligned}$$

can be determined.

A matrix can then be written

$$\begin{bmatrix} v(t_1) \\ v(t_2) \\ - \\ - \\ v(t_5) \end{bmatrix} = \begin{bmatrix} a_1(t_1) & a_2(t_1) & b_1(t_1) & b_2(t_1) & c_{11}(t_1) \\ a_1(t_2) & - & - & - & - \\ - & - & - & - & - \\ - & - & - & - & - \\ a_1(t_5) & - & - & - & c_{11}(t_5) \end{bmatrix} \cdot \begin{bmatrix} X \\ X^2 \\ Y \\ Y^2 \\ XY \end{bmatrix}$$

The inverse of the coefficient matrix which can be computed on a digital computer is then the estimator. Letting M_{ij} be the elements of the matrix inverse and because only X and Y are of interest, the solution equations are

$$\begin{bmatrix} X \\ Y \end{bmatrix} = \begin{bmatrix} M_{11} & M_{12} & M_{13} & M_{14} & M_{15} \\ M_{31} & M_{32} & M_{33} & M_{34} & M_{35} \end{bmatrix} \cdot \begin{bmatrix} v(t_1) \\ v(t_2) \\ v(t_3) \\ v(t_4) \\ v(t_5) \end{bmatrix}$$

These two equations are implemented by sampling the difference waveform at the five times t_n and multiplying the values by the M_{ij} coefficients to obtain X and Y , the parameter changes.

Many runs were taken using the procedure with several different transfer functions, testing signals and number of terms used to represent the difference waveform. The results of some of these runs are given in Table 2-2. The percentage accuracy

Table 2-2. Parameter Prediction Data

Transfer Function	Run No.	Testing Signal	Number of terms (see Eq. 2-2) linear second order cross order		Average Accuracy* %
$\frac{K}{TS+1}$	1	Square Wave	2	-	1.4
	2		2	1	1.1
	3		2	-	3.6
	4		2	1	1.2
$\frac{K}{(T_1s+1)(T_2s+1)}$ $T_1 = 4T_2$	5	Square Wave	3	-	1.9
	6		3	2	1.5
$\frac{K}{s^2+2\zeta\omega s+\omega^2}$ $\zeta = 1$	7	Square Wave	3	-	1.3
$\frac{K}{s^2+2\zeta\omega s+\omega^2}$ $\zeta = .1$	8	Square Wave	3	-	4.0
	9		3	1	1.3
	10		3	1	3.4
$\frac{KS}{s^2+2\zeta\omega s+\omega^2}$ $\zeta = 0.1$	11	Square Wave	3	1	1.3
$\frac{KS}{TS+1}$	12	Pulse	2	-	2.0
	13		2	1	1.1

* Parameter prediction average accuracy of about 30 data points with one or more parameters varying in the range of $\pm 20\%$.

given is the average of about thirty data points with one or more parameters varying within the range of $\pm 20\%$. The conclusions drawn from the data were that

- 1) The square wave was a good testing signal for lowpass and bandpass transfer functions.
- 2) The pulse was a good testing signal for highpass transfer functions.
- 3) Addition of second order terms in the equation to represent the difference waveform improved the accuracy of the parameter prediction.
- 4) Addition of cross order terms in the equation to represent the difference waveform degraded the accuracy of the parameter prediction.

In order to better understand the reasons for why poorer results are obtained when a more accurate representation is used for the difference signal waveform, the ill-conditioning of a matrix was investigated. A matrix is ill-conditioned if it is in some sense nearly singular. One measure of matrix ill-conditioning can be determined from the following (see Reference 7). The equations which the n^{th} order matrix represent can be written

$$\sum_{j=1}^n a_{ij} X_j - c_j = 0 \quad (i = 1, 2 \dots n)$$

These equations represent n hyperplanes and the angle between any two of them is given by

$$\cos^2 \theta_{ij} = \left[\sum_{k=1}^n a_{ik} a_{jk} \right] / \left[\sum_{k=1}^n a_{ik}^2 \right] \left[\sum_{k=1}^n a_{jk}^2 \right]$$

If any of the $\binom{n}{2}$ possible angles are small (say less than 15 degrees), then it is possible to have numerical stability

problems. In terms of the estimator in the single parameter testing setup, poor parameter prediction will result if any of the angles are small. Thus this technique of determining the angles between hyperplanes is a good preliminary check on whether an estimator can give a good prediction.

3.0 NONLINEAR SYSTEM TESTING ANALYSIS

The analysis in this section deals with two special nonlinearities, however, the analytical and experimental results indicate that the conclusions are applicable to a broad class of nonlinear systems. This observation is probably the most important result of the investigation because confidence in being able to measure nonlinear parameters is greatly increased if the results of an analysis of special nonlinearities can be extended to a broad class of nonlinearities. A review of nonlinear analysis in the literature led to the work by H.J. Lory, D.C. Lai and W.H. Huggins (Reference 9) which was the method of analysis which we decided to pursue.

The nonlinearities experimentally tested to establish verification of the analysis were a deadband and a soft-limiter which are in the class that can be approximated by a polynomial fit over a specified input range. These two measured nonlinearities are illustrated in Figure 3-1a and 3-1b. Figure 3-1c and 3-1d are illustrative examples of a 3rd order polynomial fit to the nonlinearity.

The problem of investigating nonlinearities can be divided into the following areas:

1. Static nonlinear elements
2. Cascaded static nonlinearities and dynamic elements
3. Feedback systems composed of nonlinear and linear dynamic elements
 - a) Nonlinearities in the feedback path
 - b) Nonlinearities in the forward path

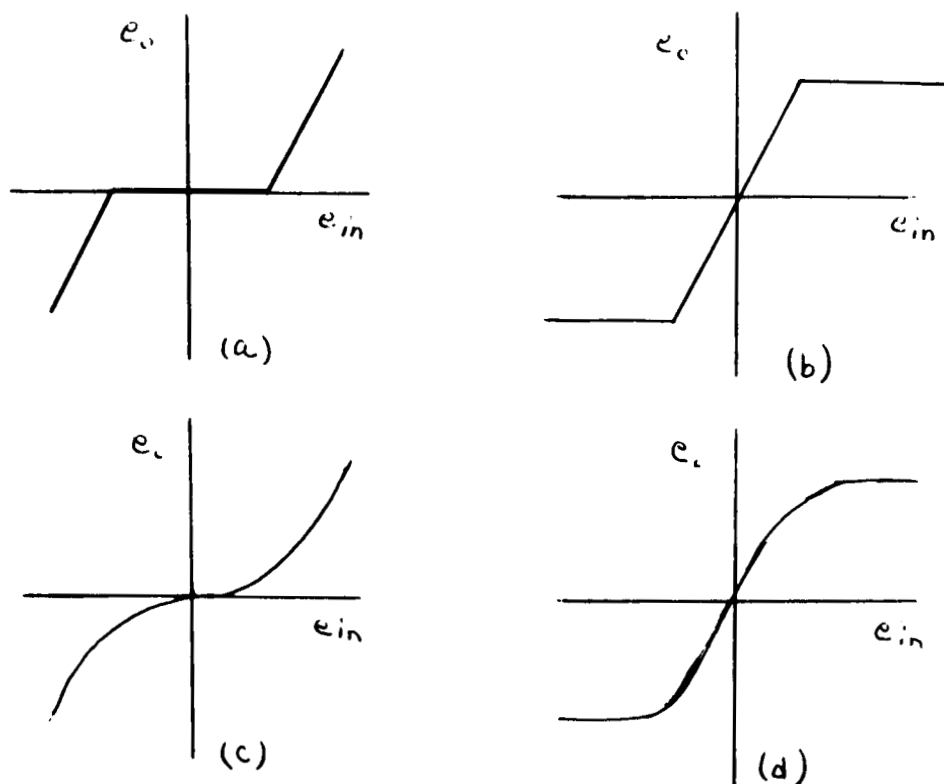


Figure 3-1
Nonlinear Elements

Each of these problems will be further defined and analyzed in the following discussions.

3.1 STATIC NONLINEAR ELEMENTS

Reference 9 is directly concerned with the identification of static nonlinear operators by using growing exponentials. The following is a brief presentation of the method reported. It is important that this method be established since it was the starting point for the work which followed on cascaded nonlinearities and dynamic systems. Assume that the static nonlinear

system can be approximated by a polynomial function of the input as

$$F(e_1) = a e_1 + b e_1^2 + c e_1^3$$

If a growing exponential signal is applied, then the output of the nonlinearity can be expressed

$$F(e_1) = a \exp(t) + b \exp(2t) + c \exp(3t)$$

Reference 9 shows that a filtering system can be constructed to perform the measurement of a , b , and c . The measured values are a minimum mean square estimate with a weighting of $1/e_1$.

Suppose we wish to measure the parameters in the sense of referencing the system to a nominal system in the single parameter testing philosophy. Under this assumption we take the Taylor series expansion and obtain the error response of

$$\Delta F(e_1) = \Delta a \exp(t) + \Delta b \exp(2t) + \Delta c \exp(3t)$$

We can now filter the error response by the same filtering system to measure the change in the parameters. The filtering is accomplished using a set of orthogonal filters as described in the Phase C Final Report (Reference 4). Figure 3-2 gives a block diagram representation of the orthogonal filter bank. The time domain representation of the filters in Figure 3-2 is:

$$\phi_1(t) = \sqrt{2} e^{-t}$$

$$= 0 \text{ for } t < 0$$

$$\phi_2(t) = 2 (-2 e^{-t} + 3 e^{-2t})$$

$$= 0 \text{ for } t < 0$$

$$\phi_3(t) = \sqrt{6} (3 e^{-t} - 12 e^{-2t} + 10 e^{-3t})$$

$$= 0 \text{ for } t < 0$$

The output of any filter $\bar{\Phi}_n(s)$ is obtained by the convolution integral

$$c_n(t) = \int_0^\infty f(t-\tau) \phi_n(\tau) d\tau$$

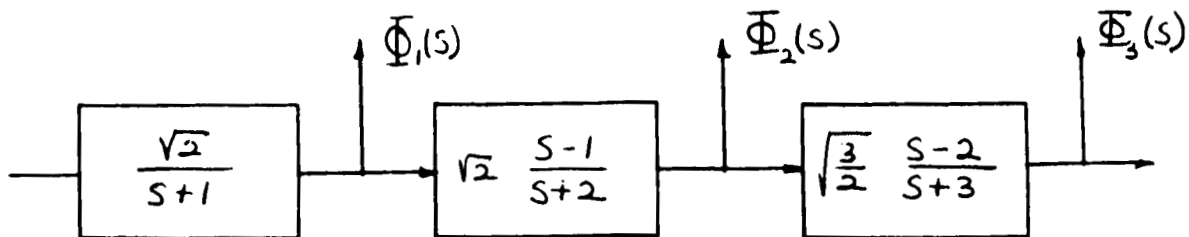


Figure 3-2

Orthogonal Filter Bank

Taking the output at time $t = 0$ and letting $t' = -\tau$ we have

$$C_n(0) = \int_{-\infty}^0 f(t') \phi_n(-t') dt'$$

and since $\phi_n(-t')$ are orthogonal over the t' interval from $-\infty$ to 0, then the output values $C_n(0)$ are the coefficients of the following series

$$f(t) = C_1 \phi_1(-t) + C_2 \phi_2(-t) + C_3 \phi_3(-t)$$

$$\Delta a e^t + \Delta b e^{2t} + \Delta c e^{3t} = C_1 \sqrt{2} e^t + C_2 2(-2e^t + 3e^{2t}) + C_3 \sqrt{6}(3e^t - 12e^{2t} + 10e^{3t})$$

By equating coefficients of the terms we have an estimator for the parameter variations of

$$\begin{bmatrix} \Delta a \\ \Delta b \\ \Delta c \end{bmatrix} = \begin{bmatrix} \sqrt{2} & -4 & 3\sqrt{6} \\ 0 & 6 & -12\sqrt{6} \\ 0 & 0 & 10\sqrt{6} \end{bmatrix} \begin{bmatrix} C_1 \\ C_2 \\ C_3 \end{bmatrix}$$

Time sampling may also be applied to measuring the parameter variations of a static nonlinearity. If we choose 3 selected sample times then the following set of equations can be used to predict the parameter variations.

$$\begin{bmatrix} \Delta a \\ \Delta b \\ \Delta c \end{bmatrix} = \begin{bmatrix} e^{t_1} & e^{2t_1} & e^{3t_1} \\ e^{t_2} & e^{2t_2} & e^{3t_2} \\ e^{t_3} & e^{2t_3} & e^{3t_3} \end{bmatrix}^{-1} \begin{bmatrix} c(t_1) \\ c(t_2) \\ c(t_3) \end{bmatrix}$$

3.1.1 Static Nonlinearity Experimentation

To verify these results by experimentation an analog multiplier was tested. The results shown in Figure 3-3 give the third order polynomial fit for the multiplier. The tests indicate that the linearity of a transfer function or any other input-output device can be tested by applying a growing exponential to the input and measuring the resulting output signal. Figure 3-4 shows example results of a linearity measurement. The function measured was a soft-limiter with the breaks at ± 50 volts. Notice that when $e_1 = 80 \text{ v}$, the equation for the function can be obtained from the data in the figure as follows:

$$\begin{aligned} 74 &= a(80), & a &= 74/80 \\ 48 &= b(80)^2, & b &= 48/(80)^2 \\ -78 &= c(80)^3, & c &= -78/(80)^3 \end{aligned}$$

Thus, the measurement of a static nonlinearity when representable by a polynomial approximation can be accomplished. If a growing exponential is applied then a linear estimator can be used to measure changes in the parameters or the magnitude of the parameters. If a known input signal is applied, time samples can also be used to establish estimates of the parameters.

3.2 CASCADED NONLINEAR AND DYNAMIC ELEMENTS

The assumption that the static-nonlinearity can be approximated by a polynomial will also be applicable to cascaded elements. The nonlinearity can be written in Laplace transform notation as:

$$H_{12}(s) = \frac{e_2(s)}{e_1(s)} = a + \frac{b \mathcal{L}(e_1^2)}{e_1(s)} + c \frac{\mathcal{L}(e_1^3)}{e_1(s)}$$

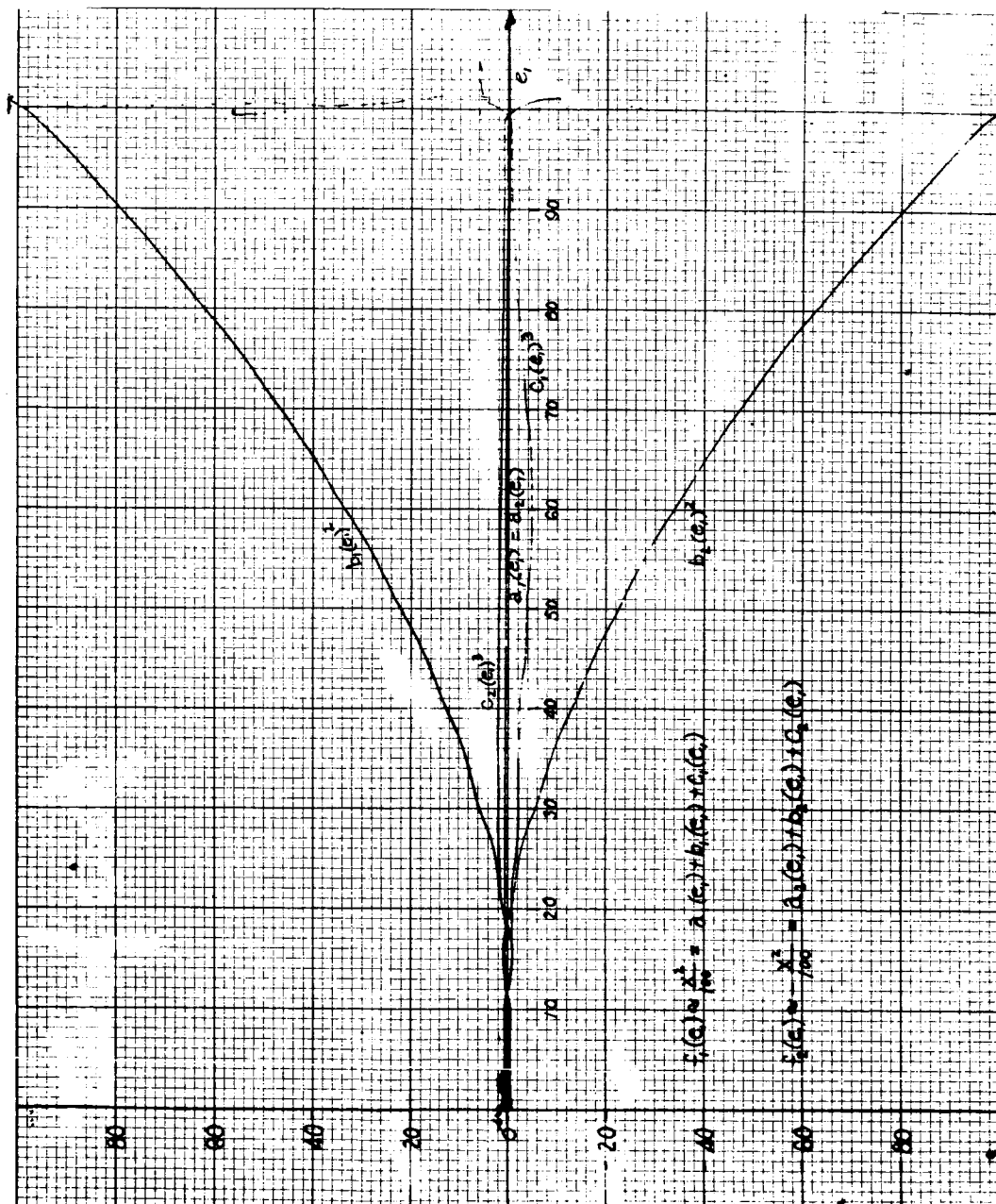


Figure 3-3. Cubic Approximation of An Analog Multiplier

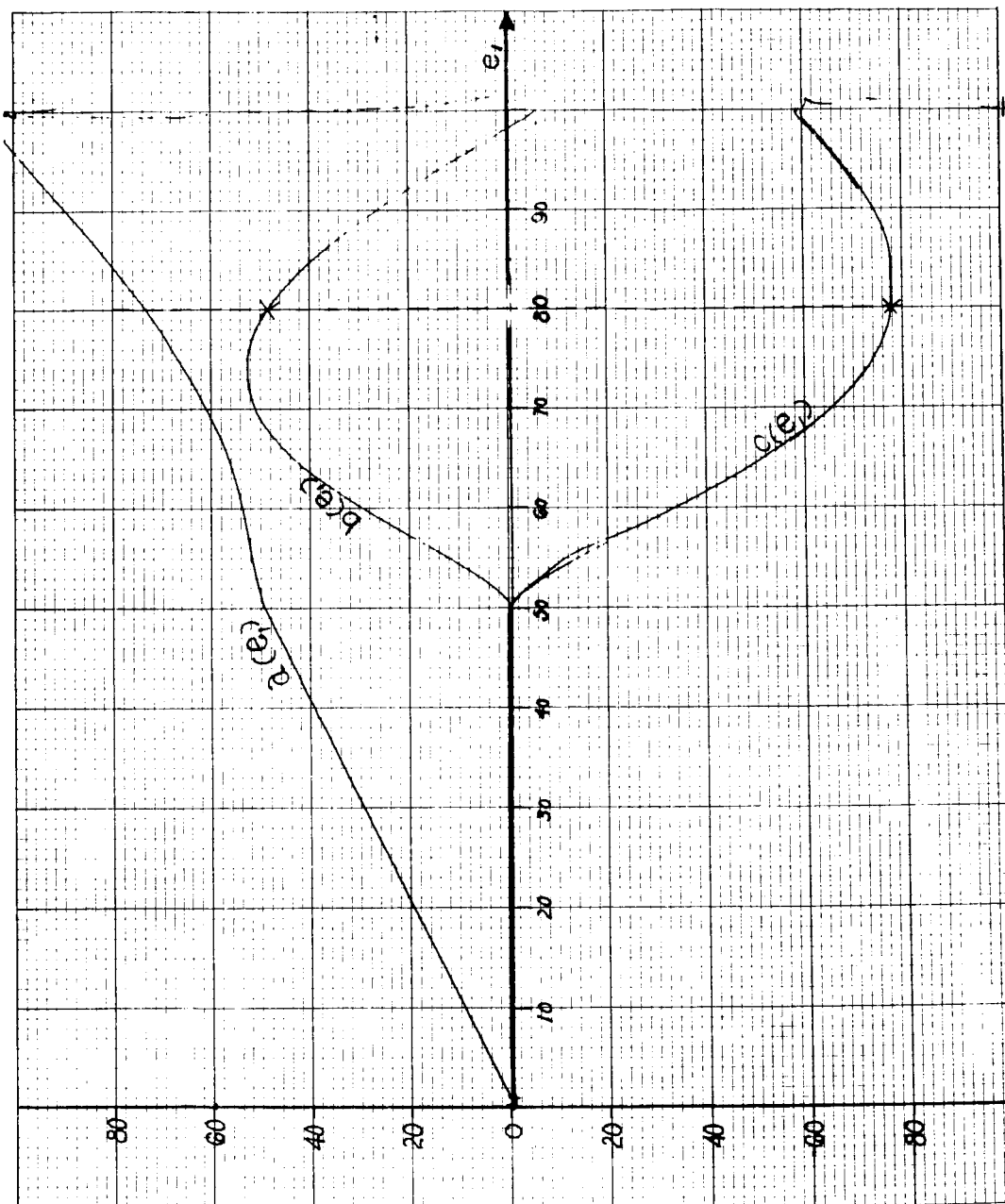


Figure 3-4. Cubic Approximation of A Soft Limiter

The total dynamic system is illustrated in Figure 3-5.

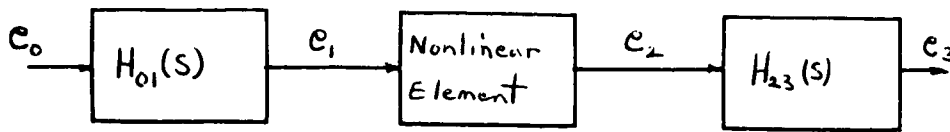


Figure 3-5

Cascaded Elements

The nonlinear element and the element transfer functions can be combined into one transfer function

$$H_{03}(s) = \frac{c_3(s)}{c_o(s)} = a H_{01}(s) H_{23}(s) + b H_{23}(s) \frac{\mathcal{L}[e_1^2(t)]}{c_o(s)} + c H_{23}(s) \frac{\mathcal{L}[e_1^3(t)]}{c_o(s)}$$

This transfer function may now be analyzed using the single parameter testing procedures developed during the first three phases. Let us assume the following example to illustrate the procedures. Let

$$H_{01}(s) = 1, \quad e_1(t) = c_o(t), \quad H_{23}(s) = \frac{1}{s + \omega}$$

The total transfer function is therefore

$$H(s) = \frac{c_3(s)}{c_o(s)} = \frac{a}{s + \omega} + \frac{b \mathcal{L}[e_o^2(t)]}{(s + \omega) c_o(s)} + \frac{c \mathcal{L}[e_o^3(t)]}{(s + \omega) c_o(s)}$$

Taking the partial derivatives with respect to the parameters a, b, c and ω for a given input signal we obtain

$$\frac{\partial H(s)}{\partial a} = \frac{1}{s+\omega}$$

$$\frac{\partial H(s)}{\partial b} = \frac{\mathcal{L}[e_o^2(t)]}{(s+\omega) e_o(s)} + \frac{\partial \left\{ \frac{\mathcal{L}[e_o^2(t)]}{e_o(s)} \right\}}{\partial b} \left[\frac{b}{s+\omega} \right]$$

$$\frac{\partial H(s)}{\partial c} = \frac{\mathcal{L}[e_o^3(t)]}{(s+\omega) e_o(s)} + \frac{c}{s+\omega} \frac{\partial \left\{ \frac{\mathcal{L}[e_o^3(t)]}{e_o(s)} \right\}}{\partial c}$$

$$\begin{aligned} \frac{\partial H(s)}{\partial \omega} = & \frac{a}{(s+\omega)^2} + \frac{b}{(s+\omega)^2} \left\{ (s+\omega) \frac{\partial \left[\frac{\mathcal{L}[e_o^2(t)]}{e_o(s)} \right]}{\partial \omega} - \frac{\mathcal{L}[e_o^2(t)]}{e_o(s)} \right\} \\ & + \frac{c}{(s+\omega)^2} \left\{ (s+\omega) \frac{\partial \left[\frac{\mathcal{L}[e_o^3(t)]}{e_o(s)} \right]}{\partial \omega} - \frac{\mathcal{L}[e_o^3(t)]}{e_o(s)} \right\} \end{aligned}$$

Two input testing signals were investigated for use in testing these cascaded elements. One was a ramp with a time base of $(1/\omega)$ seconds and the other was a pulse with a pulse width of $(1/\omega)$ seconds. Substituting the Laplace transforms of these waveforms into

the equations, the partial derivatives were determined. The partial derivatives were tested for independence by forming the Wronskian determinant and checking to see if it was zero. It was found that the ramp led to independent partial derivatives but the pulse did not.

Thus, by using a selected input signal the parameters a , b , c and ω can be measured. In general, it is reasonable to expect that the system can be tested with a large class of input signals. Although it can not be stated with assurance, we believe that any signal which is not held constant when applied to the nonlinear element should allow measurement of the factors associated with the nonlinearity when the nonlinear element is cascaded with a dynamic system.

3.2.1 Experimentation on Cascaded Elements

To verify the ability to test the parameters of cascaded elements, two nonlinearities were tested in a cascaded configuration. The systems tested were a deadband and a soft-limiter followed by a transfer function $\frac{k}{s+\omega}$. The experimental responses of the system were taken with the signal illustrated in Figure 3-6. The frequency spectrum of the signal is given in Figure 2-4.

Figure 3-7 gives the deadband system response for each of the parameter variations. The parameter variations are gain, bandwidth, and upper and lower breakpoints in the deadband element. Figure 3-8 gives the responses of parameter changes in the soft-limiter system. The parameter varied were gain, bandwidth, and

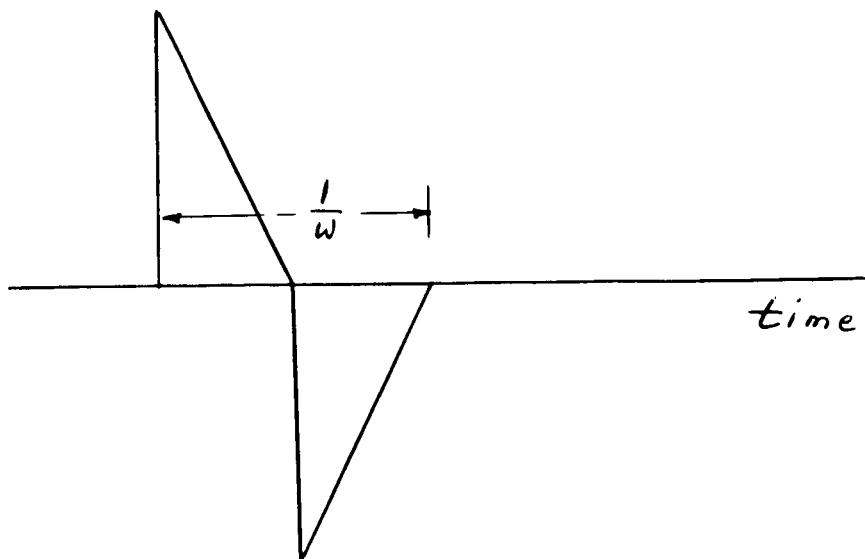


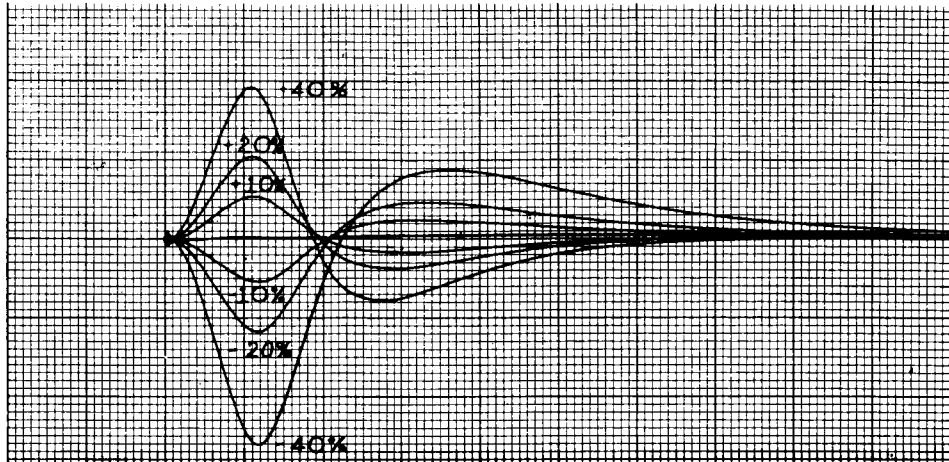
Figure 3-6
Testing Signal

upper and lower limiting levels. In all cases the parameter responses were seperable indicating independent partial derivatives.

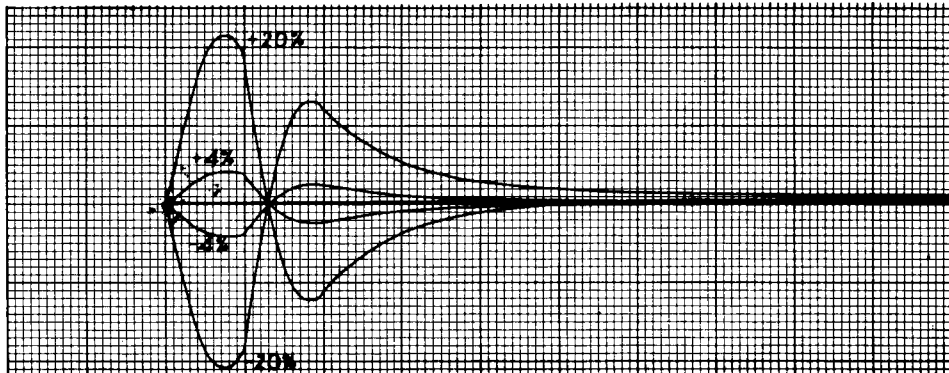
3.3 NONLINEAR ELEMENTS IN FEEDBACK SYSTEMS

Nonlinear elements in feedback systems will now be considered. We will again assume that the nonlinear element can be approximated by the cubic equation

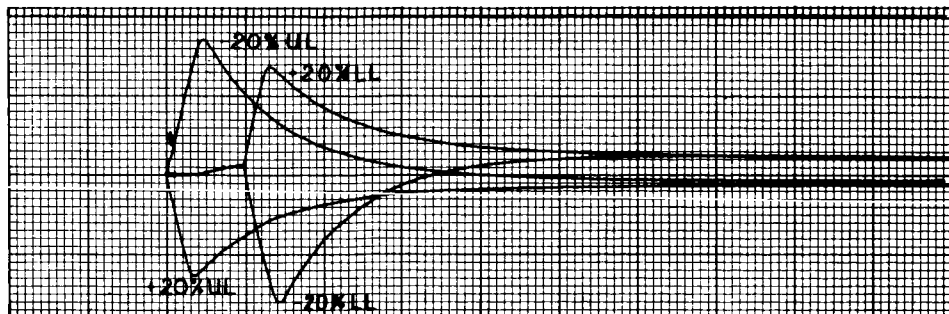
$$c_2(t) = a c_1(t) + b c_1^2(t) + c c_1^3(t)$$



Output Error Signals for Changes in (w) Dynamic Bandwidth

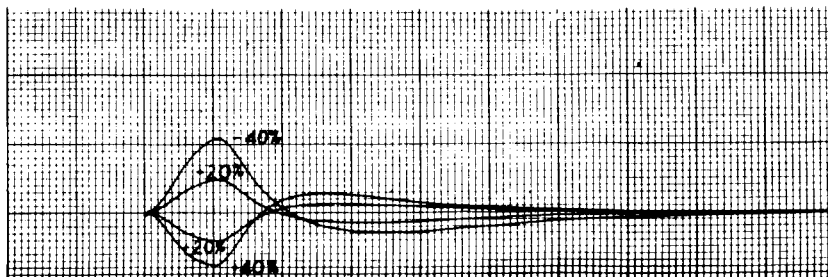


Output Error Signals for Gain (k) Changes

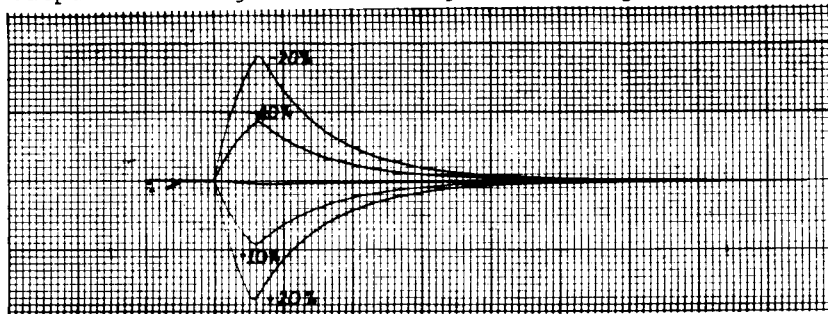


Output Error Signals for Changes in the Upper Limit (UL) and Lower Limit (LL)

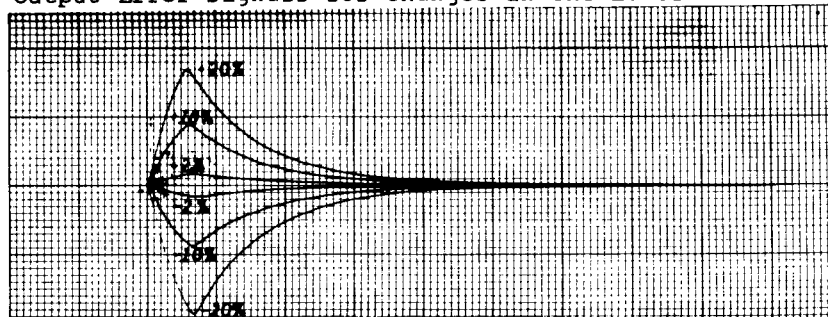
Figure 3-7. Limiter Error Response



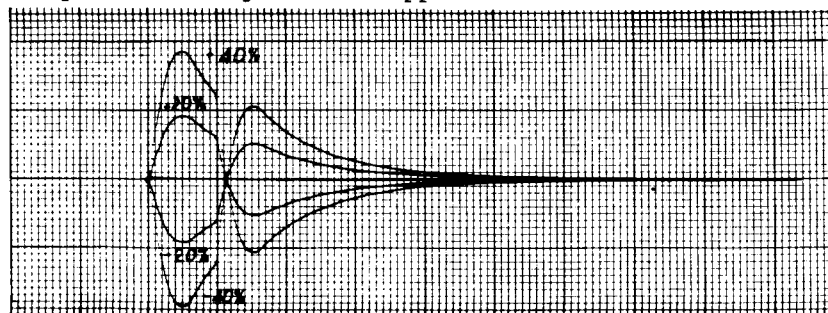
Output Error Signals for Changes in (w) Dynamic Bandwidth



Output Error Signals for Changes in the Lower Dead-band Break



Output Error Signals for Upper Dead-band Break



Output Error Signals for Gain (k) Changes

Figure 3-8. Dead-Band Error Responses

$$\frac{e_2(t)}{e_1(t)} = a + b \frac{e_1^2(t)}{e_1(t)} + c \frac{e_1^3(t)}{e_1(t)}$$

$$H_{NL}(s) = a + \frac{b \mathcal{L}[e_1^2(t)]}{e_1(s)} + \frac{c \mathcal{L}[e_1^3(t)]}{e_1(s)}$$

In feedback systems there are normally two elements, one in the feedback path, and one in the forward path as illustrated in Figure 3-9. We will first allow the nonlinearity to be the forward element and then the feedback element.

3.3.1 Nonlinear Elements in the Forward Path

The transfer function for the feedback system is

$$\frac{V_2(s)}{V_1(s)} = \frac{G_{NL}(s)}{1 + G_{NL}(s) H(s)}$$

If we assume that $H(s) = \frac{k}{s+\omega}$ then

$$\begin{aligned} \frac{V_2(s)}{V_1(s)} &= \frac{G_{NL}(s)}{1 + G_{NL}(s) \left[\frac{k}{s+\omega} \right]} = \frac{(s+\omega) G_{NL}(s)}{s+\omega + k G_{NL}(s)} \\ &= \frac{(s+\omega) \left\{ a + \frac{b \mathcal{L}[e_1^2(t)]}{e_1(s)} + \frac{c \mathcal{L}[e_1^3(t)]}{e_1(s)} \right\}}{s+\omega + a k + b k \frac{\mathcal{L}[e_1^2(t)]}{e_1(s)} + c k \frac{\mathcal{L}[e_1^3(t)]}{e_1(s)}} \end{aligned}$$

The Laplace transform of a ramp function with a time base of $(1/\omega)$ seconds was substituted into this equation and the partial derivatives of the transfer function with respect to k , ω , a , b ,

and c were determined. The partial derivatives were then tested for independence by forming the Wronskian determinant and checking to see if it was zero. It was found that the partial derivatives are independent for the case of a ramp input signal. It is important to recognize that in a practical application there will be substantial sized second partial derivatives, also, and these may limit the range over which the parameters can be measured.

3.3.2 Nonlinear Element in the Feedback Loop

The transfer function for the feedback system, assuming that

$$G(s) = \frac{k}{s+\omega} \quad \text{is}$$

$$\begin{aligned} \frac{V_2(s)}{V_1(s)} &= \frac{k/(s+\omega)}{1 + \frac{k}{s+\omega} H_{NL}(s)} = \frac{k}{s+\omega + k H_{NL}(s)} \\ &= \left\{ \frac{s+\omega}{k} + a + \frac{b \mathcal{L}[e_1^2(t)]}{e_1(s)} + \frac{c \mathcal{L}[e_1^3(t)]}{e_1(s)} \right\}^{-1} \end{aligned}$$

The Laplace transform of a ramp function with a time base of $(1/\omega)$ seconds was substituted into this equation and the partial derivatives of the transfer function with respect to k , ω , a , b , and c were determined. It was found that the partial derivative $\frac{\partial}{\partial a}$ and $\frac{\partial}{\partial \omega}$ were not independent and therefore it would be impossible to separate changes in "a" with changes in the parameter ω . Furthermore the partial derivatives with respect to these two parameters will be equal for any input signal. A parameter which could be measured was $(a-\omega)$. If, however, the

output can be taken after the nonlinearity as shown in Figure 3-9 the value of ω and could be separated since the nonlinearity is now in the forward loop.

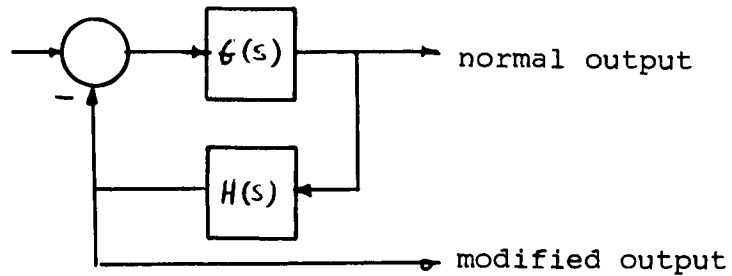


Figure 3-9

Feedback System

The point to be made is that care should be taken in the measurements of a nonlinearity to insure that the output is chosen after the nonlinearity in a feedback system, and the input signal should be of such a form as not to have constant signal levels going into the nonlinear element.

4.0 AC AMPLIFIER ANALYSIS

The analysis of the AC amplifier was divided into two parts, an experimental analysis and a theoretical analysis. The experimental analysis was done by using an actual AC amplifier and test equipment such as signal generators and oscilloscopes. A frequency plot was made on a point by point basis, measuring both magnitude and phase of the output signal with a constant amplitude input signal. The AC amplifier was then spot checked for output phase and amplitude variation from the nominal using different input signal levels.

The theoretical analysis was accomplished by using the schematic drawing and making simplifying assumptions. Then computing what the ideal transfer function would be using nominal values for the components.

4.1 EXPERIMENTAL ANALYSIS

A block diagram of the test equipment setup for the experimental analysis is shown in Figure 4-1.

Signal Generator #1 is used to generate the testing signals from 1 Hz to 10 kHz. The scope is used to detect any signal distortion in the output and the output level is measured on the rms meter.

The input signal and the output signal are used to start and stop the counter respectively, while the second signal generator

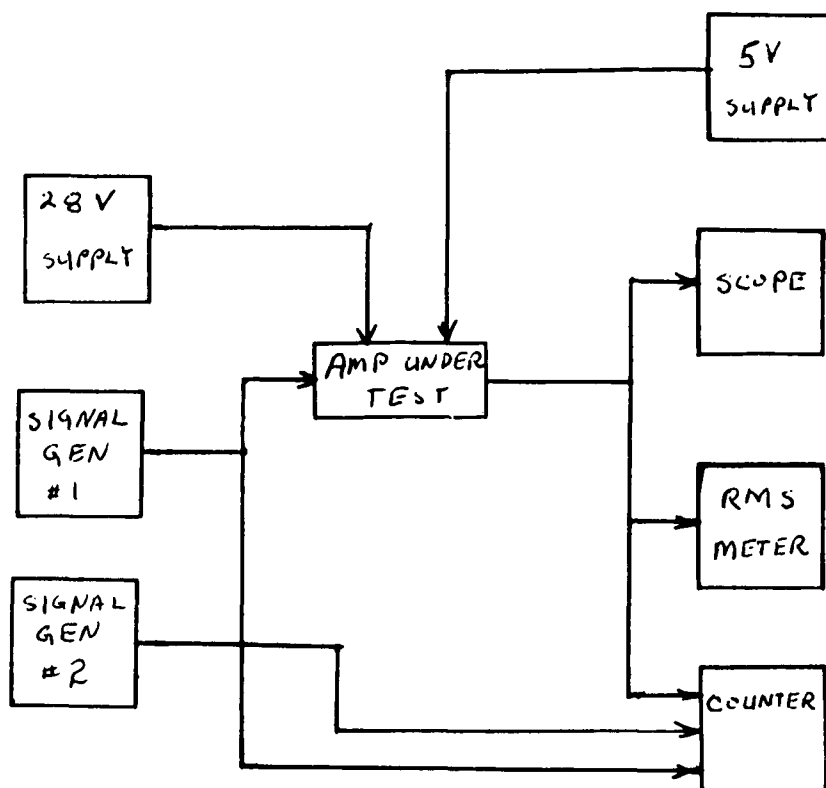


Figure 4-1

Experimental Test Setup

is set to give the proper phase indication at the given test frequency.

The amplifier was adjusted to have a gain of 100 at the midband frequency range, and this output was used as a normalized zero db signal. Figure 4-2 is a plot of the normalized output of the AC amplifier from 1 Hz to 10 kHz and Figure 4-3 is the phase plot. Since the AC amplifier had a tendency to oscillate at frequencies below 10 Hz at the given input signal level, lower signal levels were used and the output was compensated for in this range. No measurements were taken below 1 Hz due to the oscillation causing severe distortion in the output waveform.

4.2 THEORETICAL ANALYSIS

The theoretical analysis consisted of using schematic drawing number 50M04426, revision A, dated October 14, 1965 and dividing the circuit into stages which could be more easily analyzed to obtain transfer functions. One basic assumption is that the transistors can be represented by either an ideal voltage source equal to $\beta R_E I$ in the case of an emitter-follower or an ideal current source equal to βI_{in} in the case of a grounded emitter amplifier. The transistor forward current gain (β) was assumed to be 150 for the entire operating range.

The amplifier circuit analysis was divided into six stages with each division occurring at a transistor. Figures 4-4 through 4-9 are the simplified circuits for each stage of the amplifier. In the circuit for stage 6 not enough information was known about the transformer T1 to substitute circuit parameter values into the general stage transfer function. The composite transfer function is the product of each of the stage transfer functions and is equal to

$$\frac{E_o}{E_{in}} = \frac{K s^4 (s + 35.1) (s^2 + 149.5s + 227 \times 10^4) H(s)}{(s + .123)(s + 1.25)(s + 1.77)(s + 1.96)(s + 50.1)(s + 85.4)}$$

$$\frac{(s + 285.4)}{(s + 3.65 \times 10^4)(s^2 + 245.7s + 5.1 \times 10^4)(s^2 + 3.11 \times 10^4 s + 896 \times 10^6)}$$

$$\frac{}{(s^2 + 6.02 \times 10^4 s + 7.27 \times 10^9)}$$

where K is the overall amplifier midband gain and $H(S)$ is the transfer function of the output transformer stage. The two coil resistances in the third stage have been assumed to be $R_{L1} = R_{L2} = 1000$ ohms. The compensating resistor used in the third and fourth stage calculations was measured to be 320 ohms. It is estimated that the calculated poles and zeroes are accurate to within about 5 to 10% due to assumptions which have been made in parameter values and determining the stage transfer functions."

The above transfer function is plotted as a straight line Bode plot in Figure 4-10 and is normalized to zero db gain at mid-band frequencies. The similar frequency response of the theoretical transfer function and the experimentally determined frequency response in the experimental analysis indicates an accurate theoretical transfer function and also the assumption and simplifications in determining the transfer function were valid.

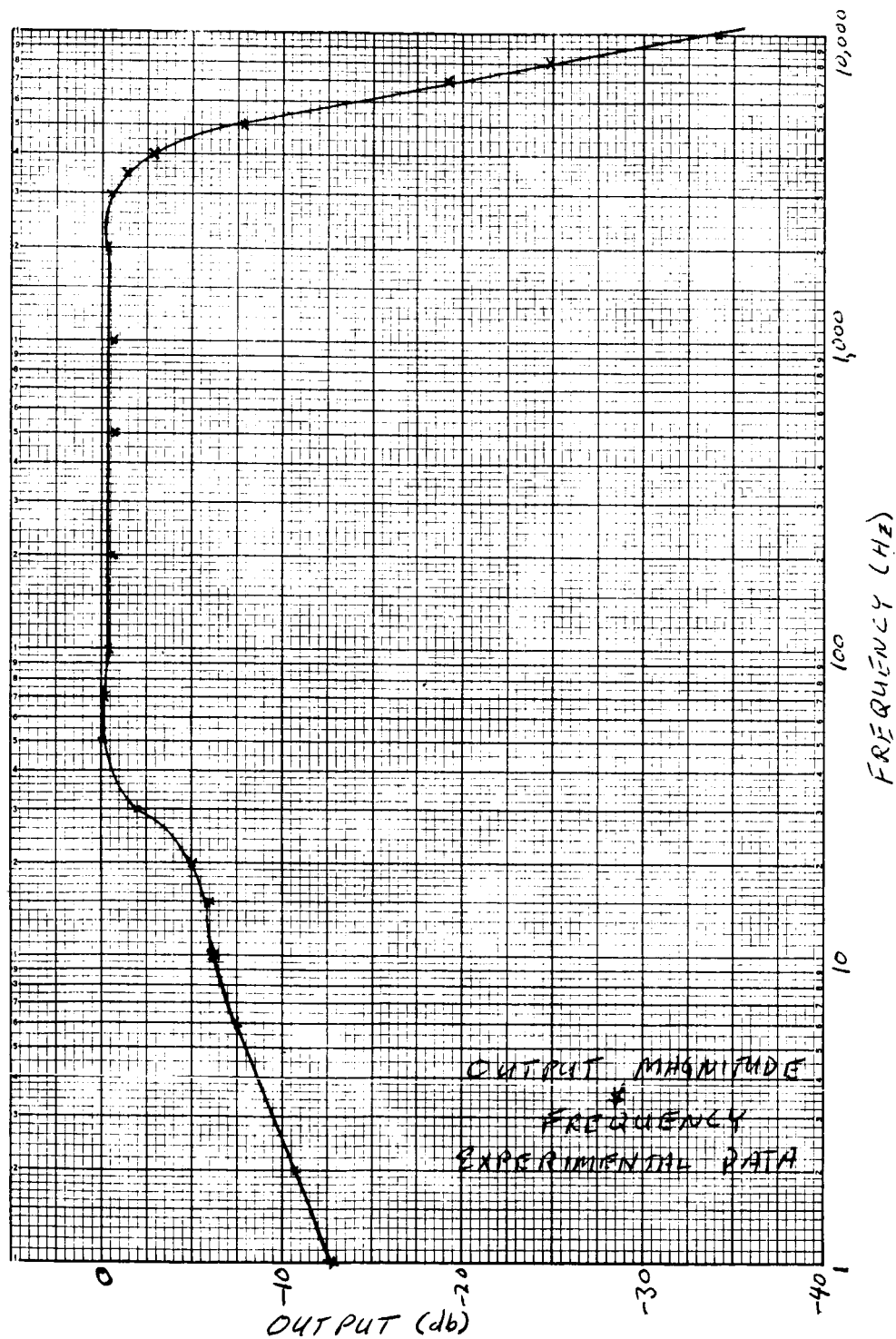


Figure 4-2. Output Magnitude and Frequency

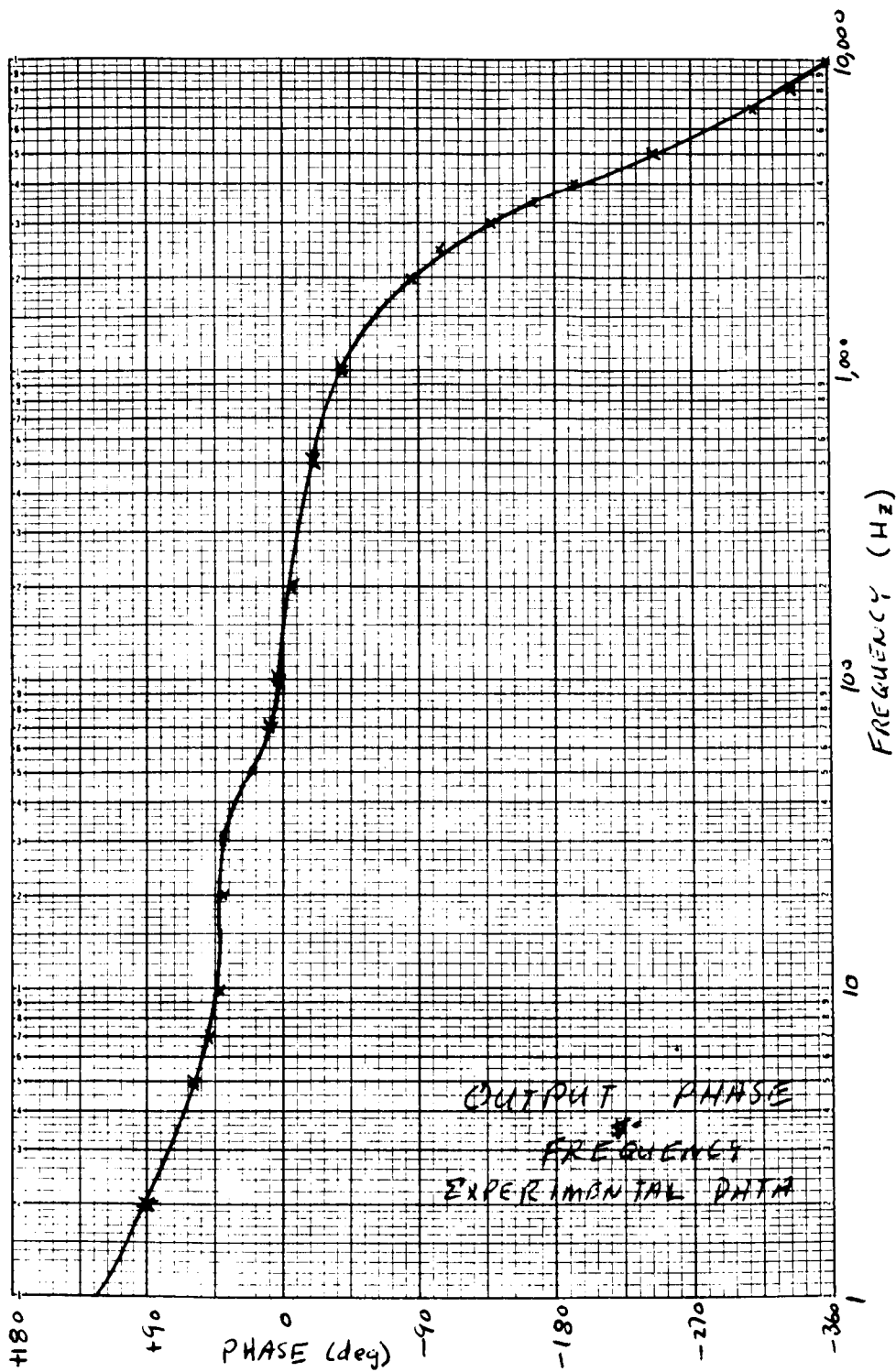
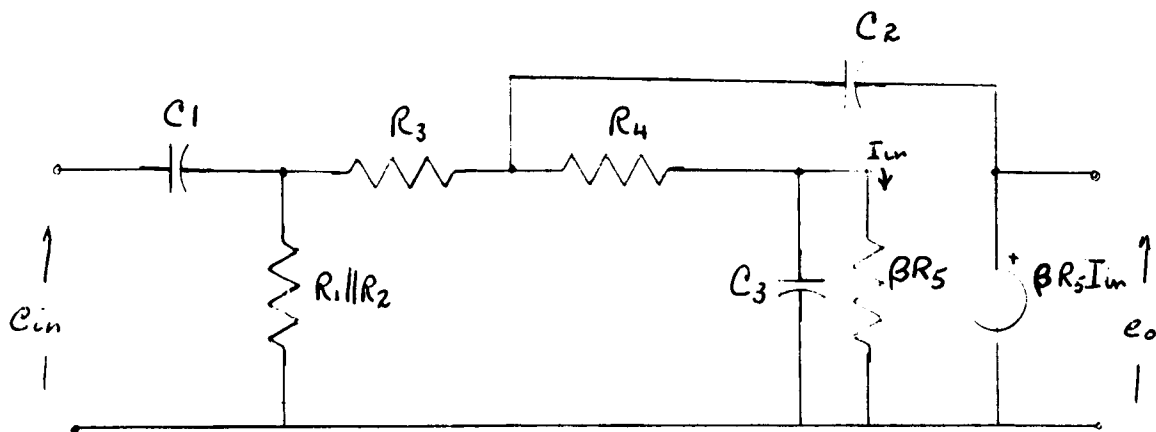


Figure 4-3. Output Phase and Frequency

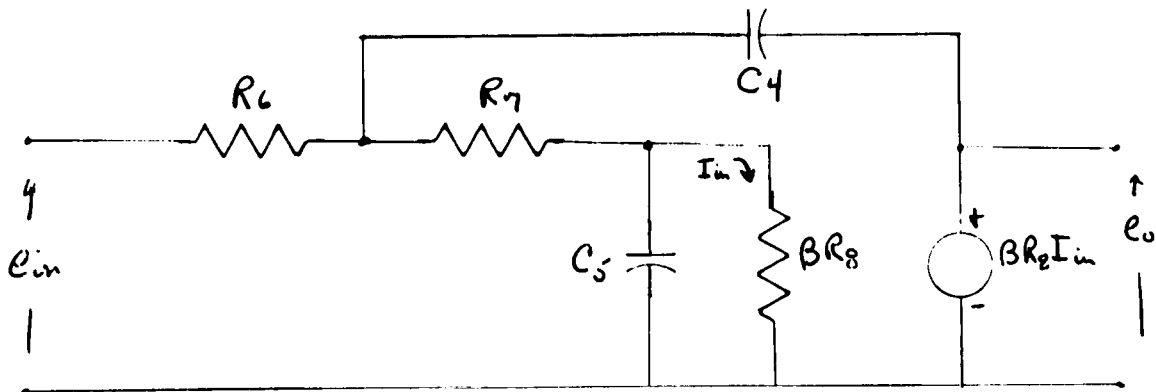


$$\frac{e_o}{e_{in}} = \frac{R_x}{\left[1 + \left(\frac{1 + \beta R_5 C_3 s}{\beta R_5} \right) (R_3 + R_4 + s C_2 R_3 R_4) \right] \left[R_x + \frac{1}{s C_1} \right] + R_x \left(\frac{1 + s \beta R_5 C_3}{\beta R_5} \right) \left(\frac{s C_2 R_4 + 1}{s C_1} \right)}$$

$$R_x = \frac{R_1 R_2}{R_1 + R_2}$$

$$\frac{e_o}{e_{in}} = \frac{-892 \times 10^9 s}{(s + .123)(s^2 + 31,100 s + 895.5 \times 10^6)}$$

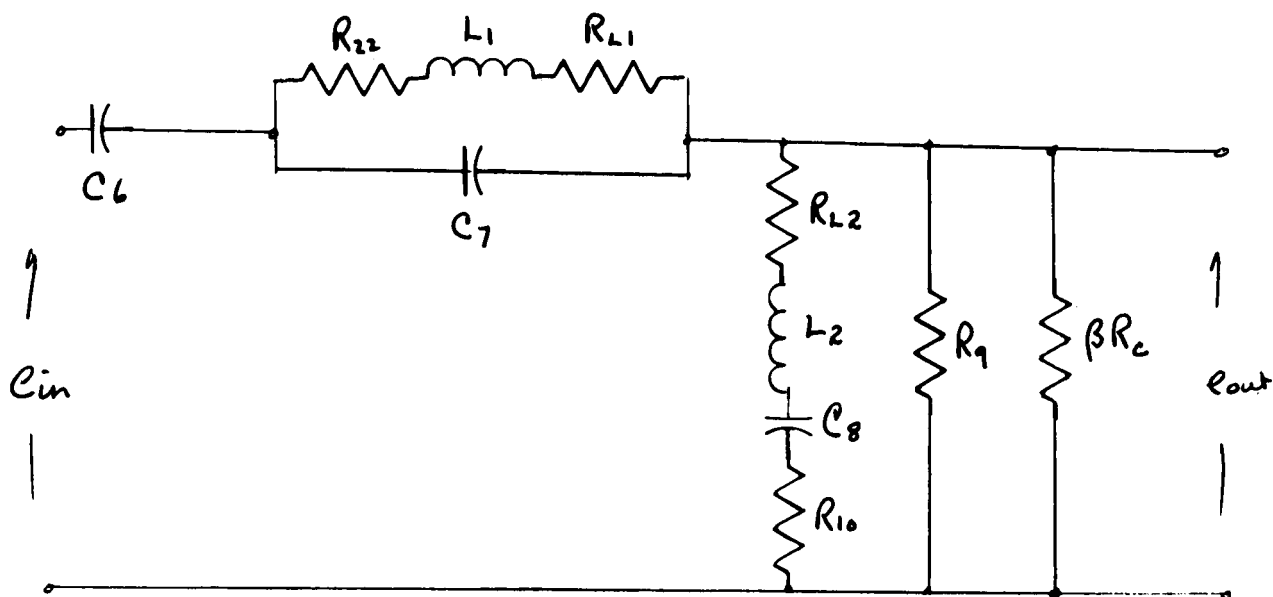
Figure 4-4. First Stage Equivalent Circuit and Transfer Unit



$$\frac{e_o}{e_{in}} = \frac{1}{1 + \left(\frac{1 + \beta R_8 C_5 s}{\beta R_8} \right) (R_6 + R_7 + s C_4 R_6 R_7)}$$

$$\frac{e_o}{e_{in}} = \frac{7.25 \times 10^9}{s^2 + 60.2 \times 10^3 s + 7.27 \times 10^9}$$

Figure 4-5. Second Stage Equivalent Circuit and Transfer Function



$$\frac{e_o}{e_{in}} = \frac{[s^2 L_2 C_8 R_{eq} + s C_8 R_{eq} (R_{L2} + R_{10}) + R_{eq}] s [s^2 L_1 C_7 + s C_7 (R_{22} + R_{L1}) + 1]}{N + [s^2 L_1 (\frac{C_6 + C_7}{C_6}) + s (\frac{C_6 + C_7}{C_6}) (R_{L1} + R_{L1}) + \frac{1}{C_6}] [s^2 L_2 C_8 + s C_8 (R_{L2} + R_{10} + R_{eq}) + 1]}$$

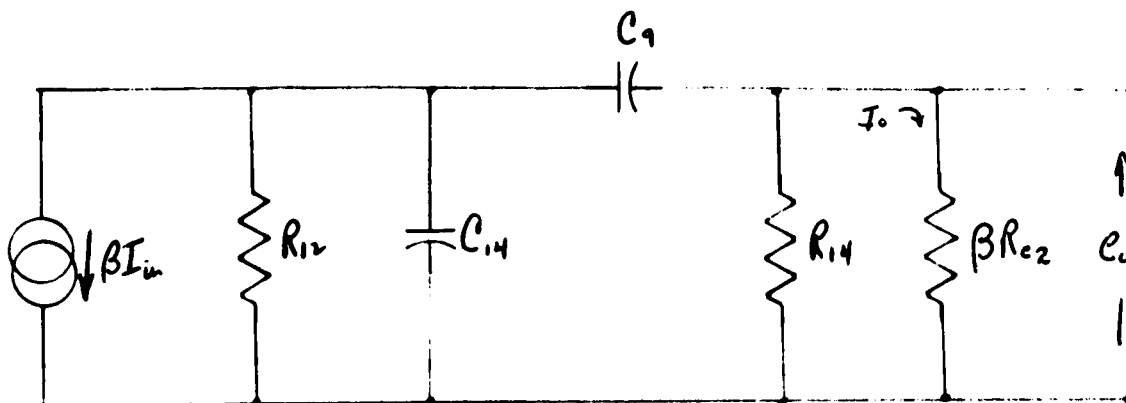
where R_c is compensating Resistor

N is Numerator

$$R_{eq} = \frac{\beta R_c R_9}{\beta R_c + R_9}$$

$$\frac{e_o}{e_{in}} = \frac{s(s+35.1)(s+285.356)(s^2 + 149.54s + 2.266 \times 10^4)}{(s+1.77)(s+50.1)(s+185.4)(s^2 + 245.7s + 5.1 \times 10^4)}$$

Figure 4-6. Third Stage Equivalent Circuit and Transfer Function

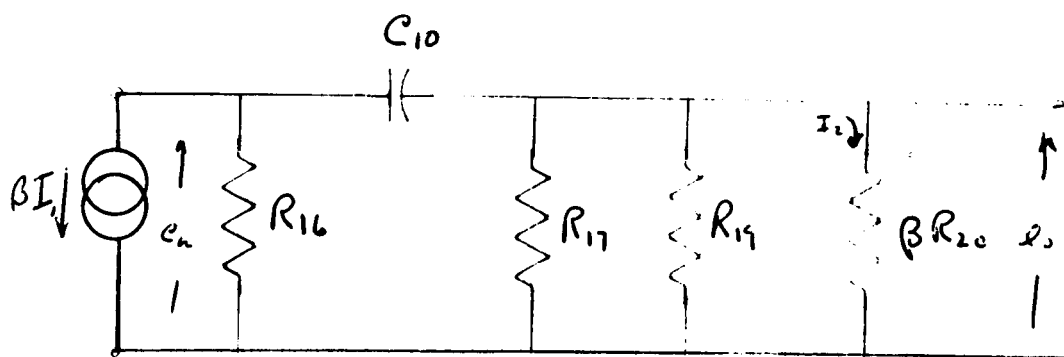


$$\frac{I_o}{I_{in}} = \frac{\beta R_{12}}{(\beta R_{c2} + \frac{\beta R_{c2} + R_{14}}{s C_9 R_{14}})(1 + s R_{12} C_{14}) + \frac{R_{12}}{R_{12}} \left(\frac{\beta R_{c2} + R_{14}}{R_{14}} \right)}$$

$$I_{in} = \frac{e_o}{\beta R_{c2}} \quad (\text{from third stage})$$

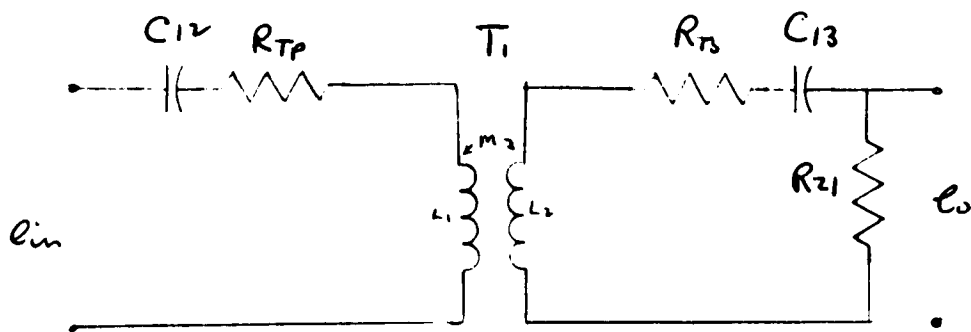
$$\frac{I_o}{I_{in}} = \frac{\frac{.553 \times 10^6}{.553 \times 10^6 s}}{(s + 1.96)(s + 36.5 \times 10^3)}$$

Figure 4-7. Fourth Stage Equivalent Circuit and Transfer Function



$$\frac{E_o}{I_1} = \frac{\beta R_{16} C_{10} R_{E4} S}{S C_{10} (R_{E4} + R_{16}) + 1} = \frac{822,000 S}{S + 1.25}$$

Figure 4-8. Fifth Stage Equivalent Circuit and Transfer Function



$$\frac{E_{out}}{E_{in}} = \frac{s^3 M R_{z1}}{s^4 (L_1 L_2 - M^2) + s^3 (L_1 R_{z1} + L_1 R_{Ts} + L_2 R_{Tp}) + s^2 \left(\frac{L_1}{C_{13}} + \frac{L_2}{C_{12}} + R_{Tp} R_{z1} + R_{Tp} R_{Ts} \right) + s \left(\frac{R_{Tp}}{C_{13}} + \frac{R_{Ts} R_{z1}}{C_{12} C_{13}} \right) + \frac{1}{C_{12} C_{13}}}$$

Figure 4-9. Sixth Stage Equivalent Circuit

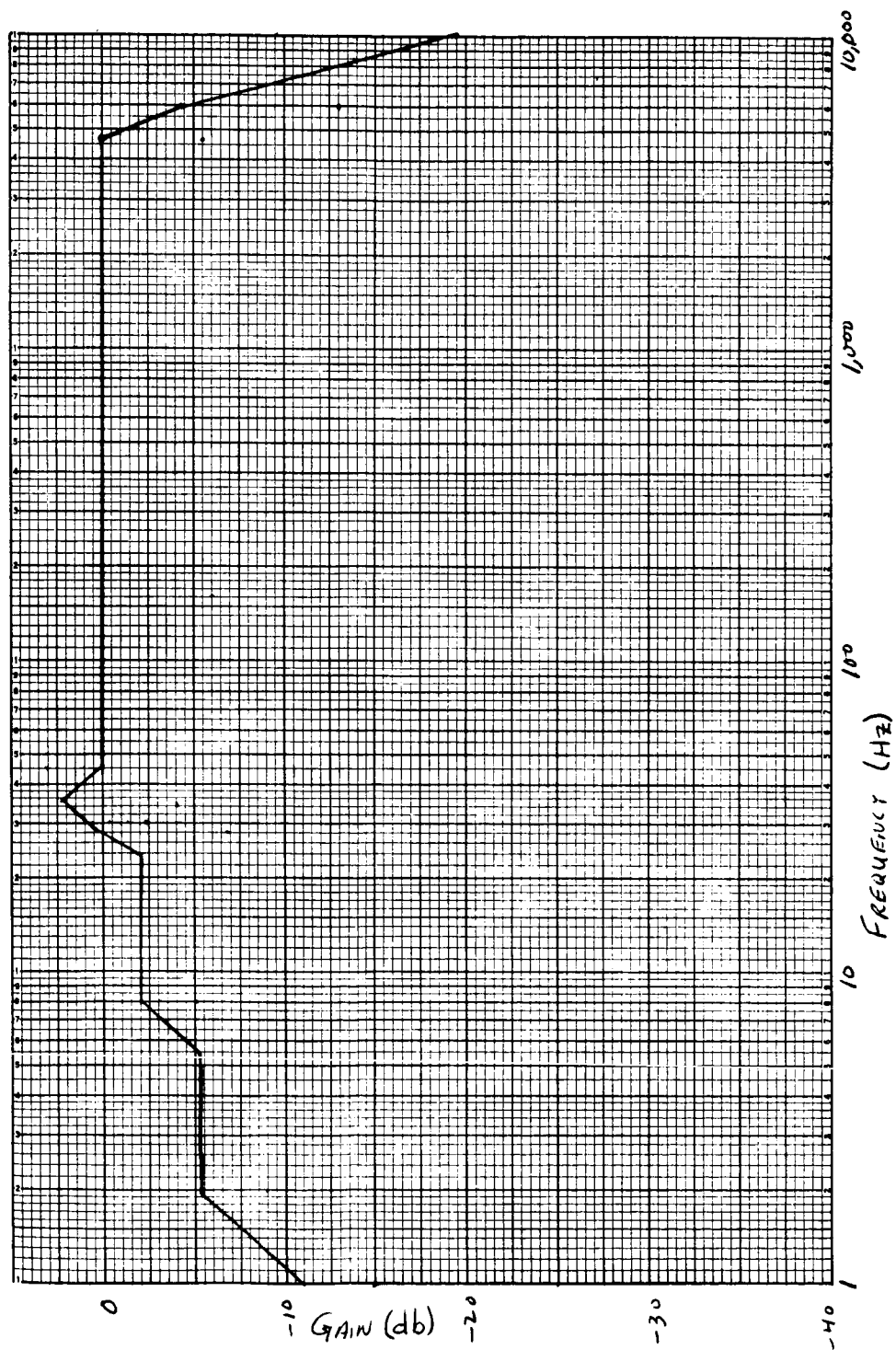


Figure 4-10. Bode Plot

5.0 TRANSFER FUNCTION DETERMINATION PROGRAM

During this quarter a digital computer program was written to calculate the transfer function of a circuit or network from the frequency-gain and frequency-phase information available by direct measurement. The output of the program is the coefficients of two polynomials, numerator and denominator, which would give a least squares curve fit to the given data.

5.1 PROGRAM THEORY

Any transfer function can be written as the ratio of two polynomials

$$\frac{\sum_{n=0}^N a_n s^n}{\sum_{m=0}^M b_m s^m} \bigg|_{s=j\omega} = \frac{C(\omega) + j d(\omega)}{C(\omega) + j f(\omega)} = M \angle \theta = \alpha(\omega) + j \beta(\omega)$$

Normalizing the denominator by letting $b_0 = 1$ and setting the real and imaginary parts equal we get the matrix equations

$$\begin{bmatrix} 1 & 0 & -\omega^2 & 0 & \omega^4 \\ | & | & | & | & | \\ | & | & | & | & | \\ | & | & | & | & | \\ | & | & | & | & | \end{bmatrix} \begin{bmatrix} a_0 \\ a_1 \\ a_2 \\ a_3 \\ a_4 \end{bmatrix} = \begin{bmatrix} \alpha & -\beta\omega & -\alpha\omega^2 & \beta\omega^3 & \alpha\omega^4 \\ | & | & | & | & | \\ | & | & | & | & | \\ | & | & | & | & | \\ | & | & | & | & | \end{bmatrix} \begin{bmatrix} 1 \\ b_1 \\ b_2 \\ b_3 \\ b_4 \end{bmatrix}$$

and

$$\begin{bmatrix} 0 & \omega & 0 & -\omega^3 & 0 \\ 0 & 0 & 0 & 0 & 0 \\ 0 & 0 & 0 & 0 & 0 \\ 0 & 0 & 0 & 0 & 0 \\ 0 & 0 & 0 & 0 & 0 \end{bmatrix} \begin{bmatrix} a_0 \\ a_1 \\ a_2 \\ a_3 \\ a_4 \end{bmatrix} = \begin{bmatrix} \beta & \alpha\omega & -\beta\omega^2 & -\alpha\omega^3 & \beta\omega^4 \\ 0 & 0 & 0 & 0 & 0 \\ 0 & 0 & 0 & 0 & 0 \\ 0 & 0 & 0 & 0 & 0 \\ 0 & 0 & 0 & 0 & 0 \end{bmatrix} \begin{bmatrix} 1 \\ b_1 \\ b_2 \\ b_3 \\ b_4 \end{bmatrix}$$

which can be combined to

$$\begin{bmatrix} 1 & \omega_x & -\omega_x^2 & -\omega_x^3 & \omega_x^4 & -\omega_x(x-\beta) & \omega_x^2(\alpha+\beta) & \omega_x^3(x+\beta) & -\omega_x^4(\alpha+\beta) \\ 0 & 0 & 0 & 0 & 0 & 0 & 0 & 0 & 0 \\ 0 & 0 & 0 & 0 & 0 & 0 & 0 & 0 & 0 \\ 0 & 0 & 0 & 0 & 0 & 0 & 0 & 0 & 0 \\ 0 & 0 & 0 & 0 & 0 & 0 & 0 & 0 & 0 \end{bmatrix} \begin{bmatrix} a_0 \\ a_1 \\ a_2 \\ a_3 \\ a_4 \\ b_1 \\ b_2 \\ b_3 \\ b_4 \end{bmatrix} = \begin{bmatrix} (x+\beta)_x \\ 0 \\ 0 \\ 0 \\ 0 \end{bmatrix}$$

or

$$[A][a] = [b]$$

where A is a matrix and a and b are vectors.

The "a" vector contains all of the unknown coefficients of the transfer function. If the number of data points is equal to the number of unknown coefficients then the A matrix is square and the coefficients can be solved for using

$$[a] = [A]^{-1}[b]$$

If more data points are used the coefficients can be solved for using

$$[a] = [A^T A]^{-1} [A^T] [b]$$

where A^T is the transpose of A. From least square statistical theory (Reference 9, 10) it can be shown that the equation gives a minimum variance estimate of the transfer function coefficients.

5.2 PROGRAM RESULTS

The program has not been fully evaluated for high order transfer functions where the phase variation is greater than ± 180 degrees, but we have evaluated the program for simple transfer functions. Using five data points corresponding to the transfer function $\frac{1}{1+s}$ the results obtained are given in Table 5-1.

Transfer function form to be fitted to the data	Transfer function determined by the program			
$\frac{a_0}{1 + b_1 s}$	a_0	a_1	b_1	b_2
	1.00434	—	1.00085	—
$\frac{a_0 + a_1 s}{1 + b_1 s}$	1.00356	7.1×10^{-4}	1.00469	—
$\frac{a_0}{1 + b_1 s + b_2 s^2}$	1.00356	—	1.00397	-7.07×10^{-4}

Runs were also made with incorrect data points and the resulting equations clearly indicated the incorrect point by showing a large deviation between the actual and calculated point. The results obtained with this program for more complicated transfer functions are still being evaluated.

6.0 CONCLUSIONS

This report documents the work performed on the single parameter testing program during the first quarter of Phase E, Contract NAS8-11715, Part III. The conclusions drawn from this effort were

- 1) Simpler to generate test signals were investigated and found to achieve single parameter testing parameter prediction results comparable to previously obtained results.
- 2) The use of second order terms to represent the difference signal between the reference system and the system to be tested, increased the accuracy of the parameter predictions. The use of cross order terms however, did not.
- 3) The transfer function of the AC amplifier was found to have a seventeenth order denominator and a twelfth order numerator. The DC amplifier will be evaluated during the next quarter.
- 4) A digital program to determine transfer functions from magnitude and phase input data was written. Initial results look good but complete program capability has not been evaluated at this time.
- 5) It was found that parameter measurements could be made of a nonlinearity represented by a polynomial, and a limiter and deadband nonlinearity.

REFERENCES

1. E.L. Berger, J.C. Jackson, "Single Parameter Testing", Phase A Report, November 1964.
2. E.L. Berger, J.C. Jackson, "Single Parameter Testing", Phase B Report, January 1965.
3. E.L. Berger, J.C. Jackson, "Single Parameter Testing", Phase C Quarterly Report, April 1965.
4. E.L. Berger, J.C. Jackson, J.T. Sterling, "Single Parameter Testing", Final Report of Phase A, B, C; August 1965.
5. J.T. Sterling, "Single Parameter Testing", Final Report Addendum, September 1965.
6. E.L. Berger, C.A. Grunden, J.T. Sterling, "Single Parameter Testing", Phase D Report, April 1966.
7. R.G. Stanton, "Numerical Methods for Science and Engineering", Prentice Hall, Inc., 1961.
8. H. Lory, D. Lai, W. Huggins, "On the Use of Growing Harmonic Exponentials to Identify Static Nonlinear Operators", IRE Transactions on Automatic Control, November 1959.
9. S. Litman, W. Huggins, "Growing Exponential as a Probing Signal for System Identification", Proceedings of IEEE, June 1963.
10. J. Kempthorne, "Design and Analysis of Experiments", John Wiley and Sons, Inc., N.Y., N.Y., 1952.